2022

Dual-ligand zinc metal organic frameworks-derived solid-electrolyte interphase for stable zinc anode in aqueous electrolytes

Penwuanna Arin
Faculty of Engineering

DUAL-LIGAND ZINC METAL ORGANIC FRAMEWORKS-DERIVED SOLID-ELECTROLYTE INTERPHASE FOR STABLE ZINC ANODE IN AQUEOUS ELECTROLYTES

Miss Penwuanna Arin

A Thesis Submitted in Partial Fulfillment of the Requirements
for the Degree of Master of Engineering in Chemical Engineering
Department of Chemical Engineering
FACULTY OF ENGINEERING
Chulalongkorn University
Academic Year 2022

วัฏภาครอยต่อระหว่างของแข็งกับอิเล็กโทรไลต์ที่ได้มาจากโครงข่ายโลหะอินทรีย์สังกะสีลิแกนด์คู่สำหรับขั้วสังกะสีที่มีเสถียรภาพในอิเล็กโทรไลต์ฐานน้ำ

น.ส.เพ็ญวรรณา อารินทร์

วิทยานิพนธ์นี้เป็นส่วนหนึ่งของการศึกษาตามหลักสูตรปริญญาวิศวกรรมศาสตรมหาบัณฑิต
สาขาวิชาวิศวกรรมเคมี ภาควิชาวิศวกรรมเคมี
คณะวิศวกรรมศาสตร์ จุฬาลงกรณ์มหาวิทยาลัย
ปีการศึกษา 2565

Thesis Title	DUAL-LIGAND ZINC METAL ORGANIC FRAMEWORKS-DERIVED SOLID-ELECTROLYTE INTERPHASE FOR STABLE ZINC ANODE IN AQUEOUS ELECTROLYTES
By	Miss Penwuanna Arin
Field of Study	Chemical Engineering
Thesis Advisor	Professor ANONGNAT SOMWANGTHANAROJ, Ph.D.
Thesis Co Advisor	Associate Professor SOORATHEP KHEAWHOM, Ph.D.

Accepted by the FACULTY OF ENGINEERING, Chulalongkorn University in Partial Fulfillment of the Requirement for the Master of Engineering

..... Dean of the FACULTY OF ENGINEERING

(Professor SUPOT TEACHAVORASINSKUN, D.Eng.)

THESIS COMMITTEE

..... Chairman

(Professor SUTTICHAI ASSABUMRUNGRAT, Ph.D.)

..... Thesis Advisor

(Professor ANONGNAT SOMWANGTHANAROJ, Ph.D.)

..... Thesis Co-Advisor

(Associate Professor SOORATHEP KHEAWHOM, Ph.D.)

..... Examiner

(PHUET PRASERTCHAROENSUK, Ph.D.)

..... External Examiner

(Assistant Professor Pornchai Bumroongsri, D.Eng.)

เพ็ญวรรณา อารินทร์ : วัฏภาครอยต่อระหว่างของแข็งกับอิเล็กโทรไลต์ที่ได้มาจากโครงข่ายโลหะอินทรีย์สังกะสีลิแกนด์คู่สำหรับขั้วสังกะสีที่มีเสถียรภาพในอิเล็กโทรไลต์ฐานน้ำ. (DUAL-LIGAND ZINC METAL ORGANIC FRAMEWORKS-DERIVED SOLID-ELECTROLYTE INTERPHASE FOR STABLE ZINC ANODE IN AQUEOUS ELECTROLYTES) อ.ที่ปรึกษาหลัก : ศ. ดร.อนงค์นาฏ สมหวังธนโรจน์, อ.ที่ปรึกษาร่วม : รศ. ดร.สุรเทพ เขียวหอม

แบตเตอรี่สังกะสีไอออนในอิเล็กโทรไลต์ฐานน้ำ (ZIBs) ได้รับความสนใจสำหรับระบบจัดเก็บพลังงาน เนื่องจากความจุจำเพาะสูง ต้นทุนต่ำ และความปลอดภัย อย่างไรก็ตาม ในอิเล็กโทรไลต์ที่มีน้ำเป็นกรดอ่อนๆ เกิดปัญหาต่างๆในด้านของสังกะสีแอโนด เช่น การก่อตัวของเดนไดรต์ และการกัดกร่อน ซึ่งจำกัดการใช้งานจริงและลดประสิทธิภาพของแบตเตอรี่สังกะสีไอออนในอิเล็กโทรไลต์ฐานน้ำ (ZIBs) โครงข่ายโลหะอินทรีย์(MOFs)คือวัสดุที่มีรูพรุนขนาดเล็กและพื้นที่ผิวภายในสูง ชั้นโครงข่ายโลหะอินทรีย์เป็นชั้นวัฏภาครอยต่อระหว่างของแข็งกับอิเล็กโทรไลต์เพื่อป้องกันไม่ให้ขั้วสังกะสีแอโนดติดโดยตรงกับตัวคั่น ในการใช้โครงข่ายโลหะอินทรีย์เป็นชั้นวัฏภาครอยต่อระหว่างของแข็งกับอิเล็กโทรไลต์เนื่องจากรูพรุนของโครงข่ายโลหะอินทรีย์ช่วยอำนวยความสะดวกในการแพร่กระจายและการขนส่งไอออนของสังกะสีได้อย่างง่ายและมีประสิทธิภาพ ในงานนี้โครงข่ายโลหะอินทรีย์ได้สังเคราะห์โครงข่ายที่มีสังกะสีเป็นโลหะแกนกลางและมีลิแกนด์เป็นกรดอิมิดาโซลและเบนซีนไตรคาร์บอกไซลิกแอซิดและไพโรไลซิสที่อุณหภูมิต่างๆ สำหรับการใช้งานแบตเตอรี่สังกะสีไอออนในอิเล็กโทรไลต์ฐานน้ำแบบรีชาร์จผลการวิจัยพบว่าขั้วแอโนดที่เคลือบด้วยโครงข่ายโลหะอินทรีย์สามารถป้องกันการกัดกร่อนจากอิเล็กโทรไลต์ได้ ในส่วนของการวัดการนำไฟฟ้าไอออนพบว่าค่าอิมพีแดนซ์ของสังกะสีแอโนดถูกลดค่าลงเมื่อถูกเคลือบด้วยโครงข่ายโลหะอินทรีย์ การทดสอบแบตเตอรี่ในระยะยาวของ Zn-BTC-Imidazole (MOFs-500°C) สามารถปรับปรุงความสม่ำเสมอของการสะสมสังกะสีบนพื้นผิวแอโนด ซึ่งนำไปสู่ความเสถียรในการทำงานของแบตเตอรี่ที่สูงขึ้นมากกว่า 600 ชั่วโมง และสามารถยืดอายุการใช้งานของแบตเตอรี่เมื่อเทียบกับสังกะสีเปล่า

สาขาวิชา วิศวกรรมเคมี ลายมือชื่อนิสิต .....

ปีการศึกษา 2565 ลายมือชื่อ อ.ที่ปรึกษาหลัก .....

ลายมือชื่อ อ.ที่ปรึกษาร่วม .....

6470395021 : MAJOR CHEMICAL ENGINEERING

KEYWORD: Rechargeable aqueous zinc-ion batteries (ZIBs), Zinc anode, Metal-organic frameworks (MOFs), Artificial solid electrolyte interphase (ASEI), Pyrolysis

Penwuanna Arin : DUAL-LIGAND ZINC METAL ORGANIC FRAMEWORKS-DERIVED SOLID-ELECTROLYTE INTERPHASE FOR STABLE ZINC ANODE IN AQUEOUS ELECTROLYTES. Advisor: Prof. ANONGNAT SOMWANGTHANAROJ, Ph.D. Co-advisor: Assoc. Prof. SOORATHEP KHEAWHOM, Ph.D.

Rechargeable aqueous zinc-ion batteries (ZIBs) have attracted attention for energy storage systems because of their high specific capacity, low cost, and safety. However, in mildly acidic aqueous electrolytes, several issues of zinc anodes such as dendrite formation, and corrosion, limit the practical deployment and performance of ZIBs. Metal-organic frameworks (MOFs) is ultrahigh porosity and high internal surface areas. MOFs layer as the solid-electrolyte interphase layer to prevent the zinc anode from attaching directly to the separator. MOFs is used in batteries as the SEI layer because the pores of MOFs efficiently facilitate the diffusion and transport of zinc-ions. In this work, MOFs having zinc as a metal ion and imidazole and 1,3,5-benzenecarboxylic acid ligands were synthesized and pyrolyzed at various temperatures for ZIBs applications. The results shows that the MOFs-coated anodes prevented the anodes and almost no change in corrosion. The impedance and ionic conductivity of zinc anode was lowered by MOFs and MOFs-X more than by bare zinc. The long-term cycle battery test of Zn-BTC-Imidazole (MOFs-500°C) can improve the uniformity of zinc deposition over the anode surface leading to higher cycling stability of more than 600 hours and extending the battery's life when compared with bare zinc anode and other works.

Field of Study:	Chemical Engineering	Student's Signature .....
Academic Year:	2022	Advisor's Signature .....
		Co-advisor's Signature .....

ACKNOWLEDGEMENTS

This research was supported by the Program Management Unit for Human Resources & Institutional Development, Research and Innovation (B16F640166)

Penwuanna Arin

TABLE OF CONTENTS

LIST OF TABLES

Page

LIST OF FIGURES

Page

Chapter I

Introduction

1.1 Introduction

Fossil fuels and coal are now employed as energy sources, which has a significant impact on air and environmental pollution and ultimately contributes to global warming. As a result, there is a growing demand for environmentally friendly renewable energy for use in electric vehicles, electronics, and battery-powered devices where energy can be stored efficiently for long periods of time. [1].

Currently, lithium-ion-based batteries are popular due to their high battery efficiency and high energy density. Although this is suitable for use in battery devices. However, lithium-ion batteries are also highly cost-constrained as lithium becomes more demanding. It is also toxic to the environment and may lead to future safety issues[2, 3].

The problems have prompted researchers to investigate at other environmentally acceptable minerals instead of lithium. The rechargeable aqueous zinc-ion batteries (ZIBs) are considered as promising alternative energy storage systems due to their large theoretical capacity (820 mAh g^{-1}). Additionally, the zinc-ion batteries (ZIBs) offer high level of safety, a large specific capacity, low cost, natural abundance, and environmental friendliness [4, 5]. However, the practical application of the zinc anode is limited by several issues such as dendrite formation, corrosion, hydrogen evolution reaction, and passivation on the surface of zinc during the charge/discharge cycle, these issues lead to ZIBs degradation, reducing coulombic efficiency, and cycling performance [6-9].

Metal-organic frameworks (MOFs) also known as porous coordination polymers (PCPs), is crystalline microporous materials, which are metal-ion and organic ligands. MOFs is ultrahigh porosity and high internal surface areas. From such properties, MOFs is used in gas storage, gas separation, liquid separation, liquid purification, catalysis, sensing, and electrochemical energy storage [10, 11]. Adding a

MOFs layer as the solid-electrolyte interphase layer to prevent the zinc anode from attaching directly to the separator. MOFs is used in batteries as the SEI layer because the MOFs is very strong porous structure. The pores of MOFs efficiently facilitate the diffusion and transport of zinc-ions. It is also useful for transporting electrons and ions to highly reversible batteries and long-life batteries [12, 13].

In this work, MOFs having zinc as a metal ion and imidazole and 1,3,5-benzenecarboxylic acid ligands were synthesized for ZIBs applications. The synthesized MOFs coated on zinc anode (MOFs@Zn) were examined by varying layer thickness and temperature for pyrolysis. The results were compared to MOFs@Zn, MOFs-X@Zn, and bare Zn anode surface leading to the high cycling stability of ZIBs and extending the battery's life.

The novelty of this work is to use two ligands in MOFs for zinc-ions batteries system. Additionally, pyrolysis is used to combine additional carbon atoms into MOFs pores, as carbon is essential for electrical conductivity, high specific capacity, and high current density. The MOFs that we created are intriguing possibilities for long-term cycle and eco-friendly batteries.

1.2 Objective

To develop dual-ligand zinc metal organic framework-derived solid-electrolyte interphase for high stable zinc anode in aqueous electrolytes.

1.3 Scope of research

1. The dual-ligand zinc metal organic framework was synthesized by using zinc nitrate with imidazole and 1,3,5-benzenetricarboxylic acid and pyrolyzed at 500°C, 600°C, 700°C, and 800°C. The anode was prepared by MOFs, Super-P, and Polyvinylidene fluoride (PVDF) as a binder with the weight ratio at 80:10:10 coated on zinc foil (thickness, 100 μm) by the doctor blading method, the thickness of the MOFs coating layer was 160 μm.
2. Glass microfiber paper as a separator.
3. The electrolyte in batteries was 2 M $ZnSO_4$ used in symmetrical cell.

4. The batteries were fabricated as CR2025 cell and measured by galvanostatic charge/discharge cycling, the coulombic efficiency (CE), electrochemical impedance spectroscopy (EIS) and material characterization were examined using field emission scanning electron microscope (FE-SEM) to examine the surface morphologies, energy-dispersive X-ray spectroscopy (EDS) to identify elements on the anode, surface area and porosity analyzer (BET), X-ray diffractometer (XRD) and X-ray absorption spectroscopy (XAS) to verify the structure, bond formation and pore size of the synthesized sample.

1.4 Research plan

Table 1 Research plan

Activities	Period											
	2022								2023			
	Jun	Jul	Aug	Sep	Oct	Nov	Dec	Jan	Feb	Mar	Apr	May
1. Literature survey and overview of the zinc anode, zinc-ion batteries, and Metal-organic framework.	■	■	■									
2. Develop coating MOFs layer of zinc anode.			■	■	■	■	■	■	■	■		
3. Test batteries performance and characterization of batteries.					■	■	■	■	■	■	■	
4. Analyze experimental results.						■	■	■	■	■	■	■
5. Write thesis and publication						■	■	■	■	■	■	■

Chapter II

Theory and Literature review

2.1 Zinc-ion batteries

2.1.1 Overview

In a zinc-ions battery, zinc-ions interact with both electrodes and transport between them via a water-based electrolyte. During discharge, zinc-ions from the anode dissolve into the electrolyte. At the same time, the cathode takes up zinc-ions from the electrolyte. Figure 2.1 shows how this process is reversed when charging [4].

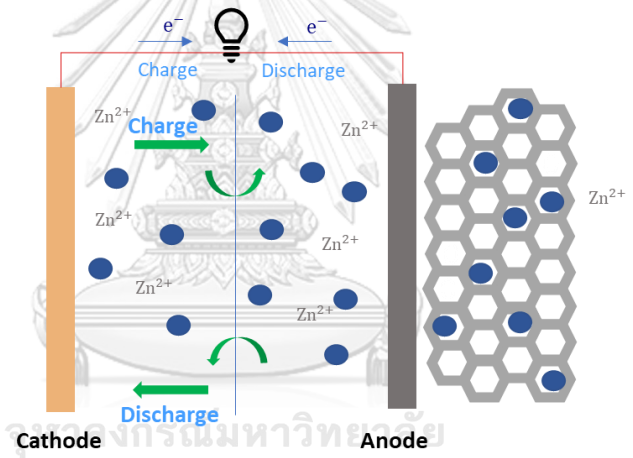

Figure 2.1 Schematic illustration of ZIBs.

2.1.2 Side reactions on the anode surface

Zinc-ions are reversibly plated or stripped on the anode surface during the charging and discharging processes of ZIBs in a mildly acidic electrolyte. Equations 2.1 and 2.2, express the zinc anode's reaction processes [9].

Stripping (discharge) : $Zn_{(S)} \longrightarrow Zn^{2+}_{(aq)} + 2e^-$ (eq 2.1)

Plating (charge) : $Zn^{2+}_{(aq)} + 2e^- \longrightarrow Zn_{(S)}$ (eq 2.2)

In mildly acidic aqueous electrolytes, several issues of zinc anodes such as dendrite formation, corrosion, and hydrogen evolution reaction, limit the practical deployment and performance of ZIBs.

2.1.2.1 Dendrite formation

Uneven electric fields, uneven distribution of ions, and infinite planar motion of surface-adsorbed zinc-ions are examples of a surface that might give rise to a zinc dendrite. The stability and useful life of zinc-containing batteries are significantly impacted by the production of zinc dendrite during charging. The probability of zinc dendrites piercing the separator and producing internal short-circuits and battery malfunction rises as they grow, especially if they have a sharp, needle-like morphology. The schematic illustration of zinc deposition and formation of zinc dendrite is shown in Figure 2.2 [6, 7].

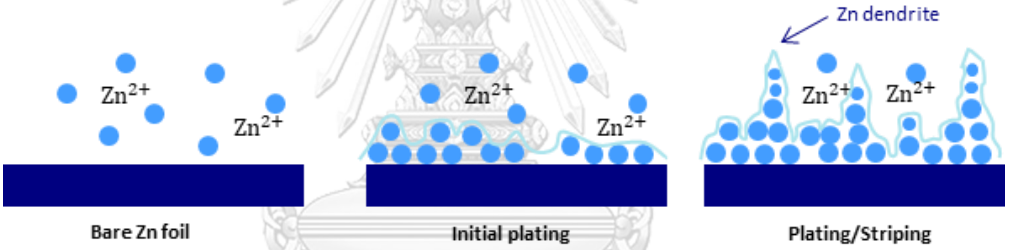

Figure 2.2 Schematic illustration of zinc deposition on bare Zn and the formation of zinc dendrite.

2.1.2.2 Corrosion reactions

The hydrogen evolution reaction (HER) is a fundamental electrochemical reaction occurring in water electrolysis to produce hydrogen. The standard reduction potential of Zn/Zn^{2+} (−0.76 V vs SHE) has a lower redox potential than hydrogen evolution potential (0 V vs SHE) and ZIBs electrolyte that is neutral or modestly acidic, zinc has a propensity to react with water and generate hydrogen bubble gas, which results in HER. Effects of HER on battery performance, such as HER reduced battery reversibility and coulombic performance. Due to the continuous use of zinc metal anodes, this reduces the efficiency and capacity of the coulombic battery, and

the H_2 gas supplied by the hydrogen evolution reaction (HER) increases the internal voltage of the battery. This causes the cells to swell and eventually explode. Their reaction mechanisms are displayed as expressed in equation 2.3 and 2.4.

Corrosion may result from hydrogen evolution reactions as shown in Figure 2.3. Electrochemical corrosion is a challenging and significant issue in the development of ZIBs. In neutral electrolyte, zinc metal corrodes quite slowly. Corrosion is accelerated by zinc metal in an electrolyte with a weak acidic content, whenever the battery is not in use. According to equation 2.3, corrosion may happen at the metal-to-electrolyte interface of zinc anode, electron acceptors in the electrolyte, like a proton or a water molecule, accept the released electrons. Thus, as seen in equation 2.4, a proton accepts electrons in order to generate hydrogen gas (H_2 gas production reaction: HER). During the charging process, hydrogen grows up in the zinc anode, causing it to expand due to increased internal pressure until it explodes and leaks electrolyte. As a result, HER in a mildly acidic aqueous ZIB electrolyte can destroy electrodes and electrolytes permanently, resulting in decreased battery life. [9, 14-17].

$$Zn \leftrightarrow Zn^{2+} + 2e^- \qquad (-0.76\ V\ vs.\ SHE) \qquad \text{(eq.2.3)}$$

$$2H^+ + 2e^- \leftrightarrow H_2 \qquad (0\ V\ vs.\ SHE) \qquad \text{(eq.2.4)}$$

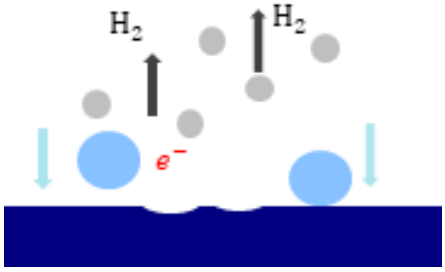

Figure 2.3 Schematic illustration of hydrogen evolution reactions (HER)

Hydrogen evolution at the anode during charging cannot be prevented, and extra OH^- will be produced on the surface electrode. Along with interacting with Zn^{2+}

to create zinc oxide and passivate the electrode surface, OH^- will also directly react with zinc to cause corrosion of the metal and produce hydrogen. Equations 2.5 and 2.6 illustrate the reactions.

$$Zn^{2+}+4OH^- \leftrightarrow Zn[(OH)_4]^{2-} \leftrightarrow ZnO+H_2O+2OH^- \quad \text{(eq.2.5)}$$

$$Zn+2OH^-+2H_2O \longrightarrow Zn[(OH)_4]^{2-}+H_2 \quad \text{(eq.2.6)}$$

The concentration of Zn^{2+} near the anode will rise because of the metal zinc converting to Zn^{2+}which will lead to anions and cations combining to produce zinc oxide and zincate, which will passivate the electrode surface due to migration.

The appearance of hydrogen evolution would be made worse by the rapid expansion of the anode caused by dendrite formation on a particular surface area. In contrast, passivation, and corrosion lead to an uneven zinc anode surface, which promotes dendrite formation. As a result, the problems with the anode are related and mutually reinforcing. Therefore, if one issue is completely fixed, the others will follow suit in a reasonable manner. [14, 17, 18].

2.2 Metal-Organic Frameworks (MOFs)

Metal-Organic Frameworks (MOFs) are crystalline porous organic-inorganic hybrid materials produced by an arrangement of positively charged metal ions surrounded by organic "linker" molecules. The metal ions perform as nodes, combining the branches of the linker to generate a recurrent, cage-like structure. Ultrahigh porosity (90% free volume) and high internal surface areas are MOFs distinguishing structural characteristics. The properties of MOFs are used to gas storage and separation, catalysis, sensing, and electrochemical energy storage [10, 11].

2.2.1 Artificial solid electrolyte interphase (SEI)

Pu et al. reported the zinc anode's ability to cycle when coated with ZIF-8 (Zeolitic imidazolate framework-8), which has metal zinc and imidazole ligand. It was characterized in symmetrical ZIF-8@Zn||ZIF-8@Zn coin cells based symmetric cells with 2 M $ZnSO_4$ electrolyte at a current density of 0.25 mA cm^{-2} and a charge/discharge capacity of 0.05 mAh cm^{-2} as shown in Figure 2.4. It was reported that zinc anodes coated with ZIF-8 produced longer cycling performance than bare Zn. The ZIF-8@Zn has a greater cycle life at 170 hours than the bare Zn, which short circuits after 20 hours [13].

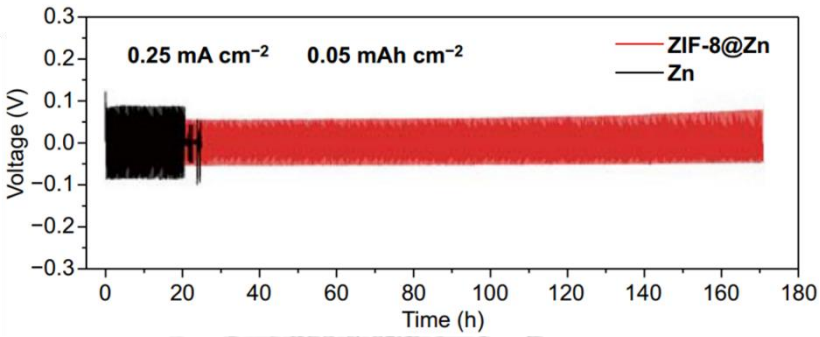

Figure 2.4 The cycling performance of symmetrical cells with bare Zn and ZIF-8@Zn electrodes 2 M $ZnSO_4$ electrolyte at current density is 0.25 mA $cm^{-2}$with zinc capacity of 0.05 mAh cm^{-2}. [13]

The evolution of the morphology of the ZIF-8@Zn electrode and the bare Zn electrode by SEM before and after 100 charge/discharge cycles. The surface of the zinc foil generates several large protuberances after cycling, as shown in Figure 2.5a, b indicating an uneven process of zinc stripping/plating during repeated charge/discharge cycles.

The ZIF-8@Zn electrode has a porous ZIF-8 coating on it, as shown in Figure. 2.5c and after cycling as shown in Figure. 2.5d, no large dendrites are visible. After 100 cycles, the ZIF-8 layer is still adhered to the zinc foil, which means the ZIF-8 coating is stable in ZIBs.

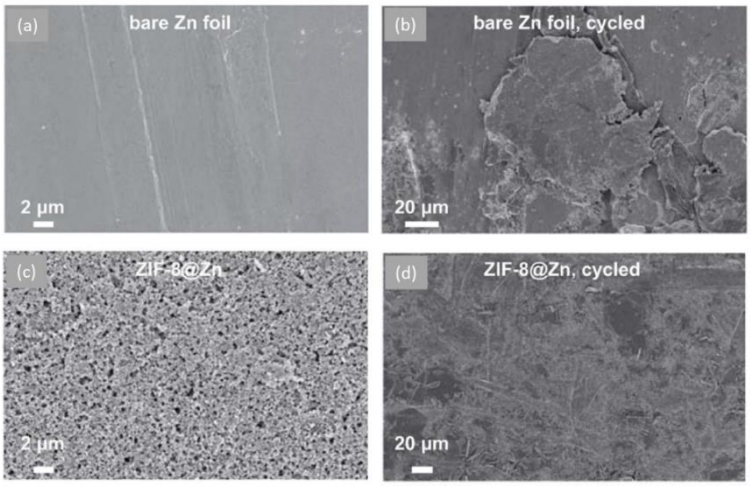

Figure 2.5 SEM images of bare Zn (a.) before and (b.) after 100 stripping/plating cycles, ZIF-8@Zn (c.) before, and (d.) after 100 stripping/plating cycles. [13]

Figure 2.6 shows a schematic representation of the morphological change of bare Zn and ZIF-8@Zn electrodes after repeated zinc stripping and plating. Zinc prefers to deposit at specific areas during plating and form small protuberances and dendrites. Due to the unbalanced electric field created by these small dendrites, Zn^{2+} is likely to be drawn to it and generate uncontrolled dendrites. The porous ZIF-8 coating on the ZIF-8@Zn electrodes can homogenize the zinc-ions flux, preventing an unequal distribution of the electric field and inhibiting dendrite formation.

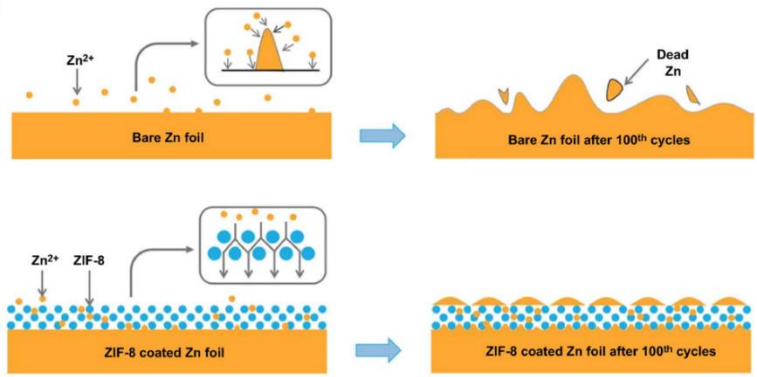

Figure 2.6 Schematic illustration for the morphology of the bare Zn and ZIF-8@Zn electrodes during zinc stripping/plating. [13]

Wang et al. demonstrated the cycling efficiency of zinc anode coated Zn-BTC, which was characterized in symmetrical Zn-BTC@Zn||Zn-BTC@Zn coin cells based symmetric cells with 2 M $ZnSO_4$ electrolyte at 3 mA cm^{-2} with 0.5 mA h $cm^{-2}$and 4 mA $cm^{-2}$with 1 mAh cm^{-2}. Figure. 2.7a and b shows that the coated anode-based symmetric cell demonstrated lower polarization than bare Zn in both conditions, suggesting that the coated Zn-BTC allowed for controlled access of Zn^{2+} to the electrode surface. At current densities of 3 mA cm^{-2} and 4 mA cm^{-2}, the symmetric cells with coated anodes showed stable cycling for 400 hours while their counterparts with bare Zn anodes short-circuited after roughly 154 and 81 hours [19].

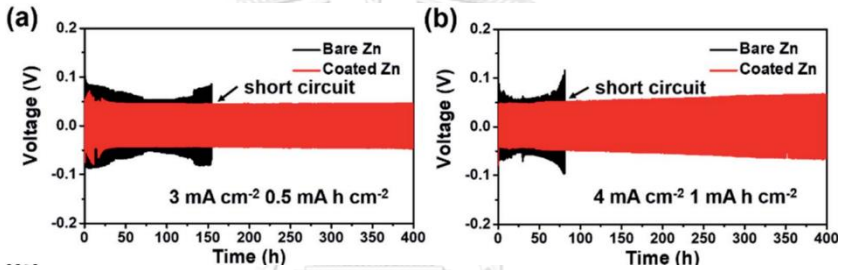

Figure 2.7 Cycling performance of symmetrical cells with bare Zn and coated zinc anodes at the current density of (a.) 3 mA cm^{-2} with a capacity of 0.5 mAh $cm^{-2}$and (b.) 4 mA $cm^{-2}$with a capacity of 1 mAh cm^{-2}. [19]

The SEM images of the before and after-cycling electrodes with the Zn–BTC layer and bare Zn were collected and compared (Figure. 2.8). The bare Zn surface deteriorated after cycling at 0.4 mA cm^{-2} with 0.1 mA h cm^{-2}, showing a difference in morphology from smooth to rough. In contrast, coated zinc can keep a uniformly smooth surface. The diffusion and uncontrolled deposition of Zn^{2+} led to uneven zinc deposition and dendrite formation on bare Zn.

To investigate the corrosion resistance property of the Zn-BTC layer, the bare Zn and Zn-BTC were immersed in 2 M $ZnSO_4$ electrolyte. The bare Zn corroded and turned dark grey after several days of immersion, as seen in Figure. 2.9a. The coated anode changed almost nothing after immersion. SEM showed the micro-

morphologies of the Zn-BTC and bare Zn after being submerged in the 2 M $ZnSO_4$ electrolyte. As seen in Fig. 2.9b, several by-products resembling regular hexagonal flakes were found on the bare Zn surface as compared to the initial surface. The performance is known to be dependent on the passivating SEI coating that forms on the anode during cycling. The electrolyte's corrosion of the flexibly and randomly organized by-products results in the eroded formation of bare Zn with no useful protective layer (e.g., SEI film), resulting in reduced battery performance. Due to the lack of byproducts, it efficiently reduces the electro-corrosion of the zinc anode as compared to Zn-BTC (Figure 2.9b). In other words, the coating layer made of Zn-BTC and a PVDF binder functions as an artificial SEI film to protect the anode and the electrolyte from being in direct contact and slow down on the production of byproducts.

It can be concluded that the SEI layer can improve the efficiency of the anode by preventing the formation of zinc to form dendrites and preventing electrolyte corrosion on the anode.

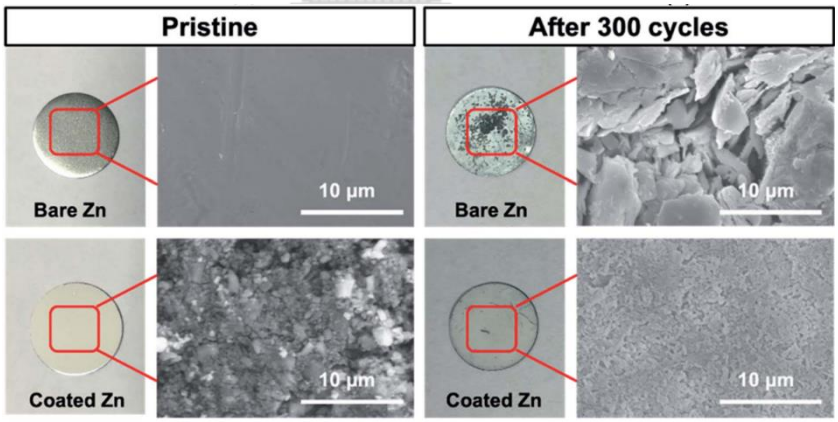

Figure 2.8 Photographs and SEM images of the different anodes before and after 300 cycles at a current density of 0.4 mA cm^{-2} with a capacity of 0.1 mAh cm^{-2}. [19]

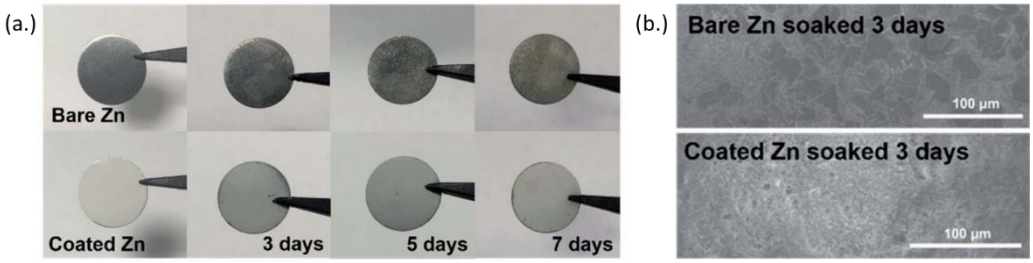

Figure 2.9 (a.) Photographs and (b.) SEM images of bare Zn and Zn-BTC soaked in a 2 M $ZnSO_4$ electrolyte for different periods [19]

The long-term cycle stability of MnO_2||Zn-BTC and MnO_2||bare Zn were also tested at current density of 2000 mA g^{-1} to measure the effect of the coating strategy (Figure. 2.11a). The cells with different anodes initially showed comparable decay tendencies and a specific capacity of 140 mAh g^{-1}. The cell with Zn-BTC had significantly improved cycling stability after 50 cycles, with a capacity of 116.6 mAh $g^{-1}$and a retention rate of 81.1% at the 1000th cycle [19].

As a result, it can be said that using MOFs as the SEI layer can lessen dendritic formation, corrosion, and hydrogen evolution reaction from plating and stripping. Consequently, it can increase the battery life for a long-life cycle.

Yin et al. study the high-performance two ligands of MOFs-based cathodes for ZIBs, which has manganese as metal and the ligand were imidazole and 1,3,5-benzenetricarboxylic acid. The ex-situ XRD was used to examine the structural evolution at various reaction states of the Zn^{2+} ion storage mechanism of Mn-H_3BTC -MOF-4. According to the second cycle's ex-situ XRD patterns of Mn-H_3BTC -MOF-4 electrodes (Figure. 2.10), the shift of the peaks can be slightly seen during the charging/discharging process. This suggests that the structure of Mn-H_3BTC-MOF-4 has developed in a highly reversible. Another aspect shows that the Mn-H_3BTC -MOF-4 is stable all through the electrochemical process. The long-term cycle stability of Mn-H_3BTC-MOF-4||bare Zn was tested at a high current density of 3000 mA g^{-1}. The Mn-BTC-MOF-4 cathode displays a specific capacity of 97 mAh g^{-1} and retention rate of retaining 93.5% of its initial capacity after 1000 cycles, along with 93.5% coulombic

efficiency. Wang et al. demonstrated the long-term cycling with MOFs single ligand (Only H_3BTC) at a current density of 2000 mA g^{-1} the long-term cycling performance is unstable (Figure. 2.11a) [19] when compare with two ligand (Mn-H_3BTC-MOF-4) from Figure. 2.11b, the graph is quite stable because of MOFs structure. Two ligands of MOFs make the structure of MOFs coagulated to be stronger and more stable. As a result, the stability of the MOFs results in a long-term cycling performance of batteries[20].

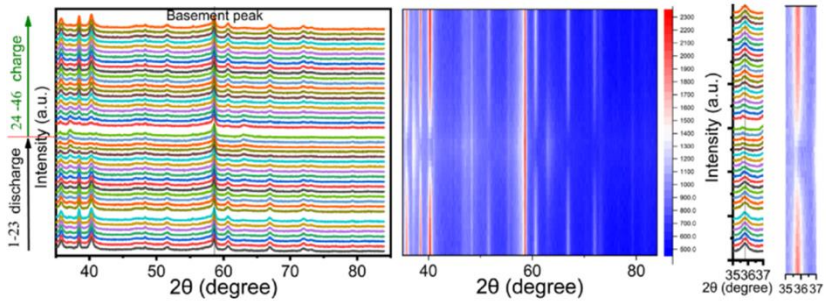

Figure 2.10 Ex-situ XRD patterns of cycled electrodes at different charged/discharged stages[20].

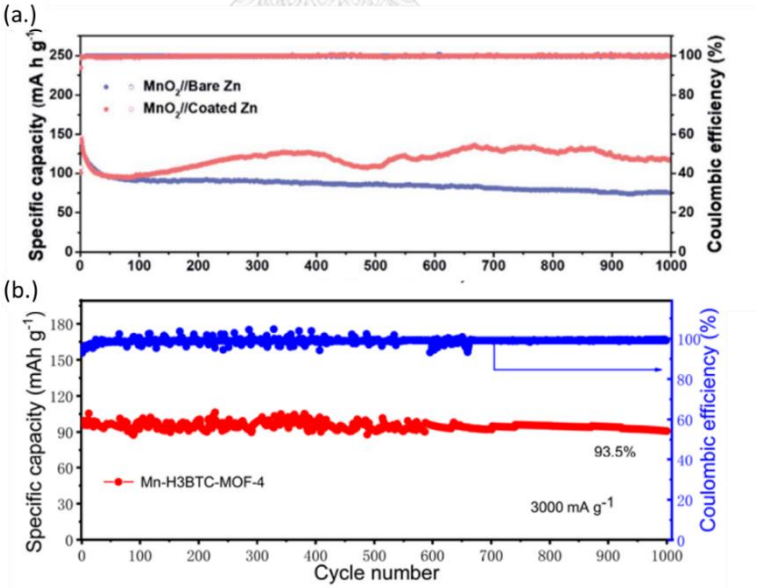

Figure 2.11 (a.) Long-term cycling performance at a current density of 2000 mA g^{-1} [19]. and (b.) cycling performance of Mn-H_3BTC-MOF-4 at a current density of 3000 mA g^{-1} [20].

Sharma et al. study the dual ligands of MOFs-based anode for LIBs, which has iron as metal and the ligand were terephthalic acid and naphthalene dicarboxylic acid[21]. In addition Baskoro, Ngue et al., study the dual ligands of MOF-based anode for LIBs, which has zinc as metal and the ligand were tris(4-(1H-1,2,4-triazol-1-yl)phenyl)amine (TTPA) and dihydroxylterepthate(DHTP) [22].Both studies examined the ion reversibility and stable structure of the anode. As a result, the dual ligand is highly reversible and has a higher capacitance. By having dual ligands, the pore size is not too large, there is a limited surface area. The MOFs pores are like a grille, resulting in a uniform distribution of ions and reducing the formation of dendrites[21, 22].

The design of the MOFs material is an important step because the suitable selection of metal centers and connection between ligands leads to a specific crystal structure with specific pore size properties. MOFs are resilient substances both chemically and physically. However, there are worries regarding the amount of metal discharged into the environment in the event of depreciation or breakdown. Therefore, it is preferred to synthesize MOFs using metal ions with minimal toxicity, such as alkaline-earth metals (Mg or Ca) or Mn, Fe, Al, Ti, and Zn [23]. Zinc is an attractive choice due to its low cost, low toxicity, and a good host for the anode. The host zinc for the anode is a magnet-like sucker to attract ions in an orderly manner and side problems such as dendrites can be avoided. The carboxyl groups and N atoms in the organic ligands provide them with more complicated and varied coordination modes. Between the aromatic rings, there are additional H-bond and $\pi-\pi$ stacking effects. Because of the free carboxyl groups and coordinating water molecules present in these ligands, proton conduction can be significantly assisted by their appearance. Many of the O atoms in the 3D framework can also potentially facilitate H-bonded networks that profit from proton transfer [24, 25].

2.2.2 Pyrolysis

Wang et al. shows the as-prepared ZIF-8 was pyrolyzed at various temperatures (400 ℃, 500 ℃, 600 ℃, and 800 ℃). The plating and stripping performances of these samples (i.e., ZIF-8-400, 500, 600, and 800) in 2 M $ZnSO_4$ electrolytes were evaluated at a capacity of 1.0 mAh cm^{-2} and current density of 2.0 mA cm^{-2}. The ZIF-8-500 electrode has substantially higher plating and stripping reversibility than other electrodes, as shown in Figure 2.12A and highly stable coulombic efficiency of 98.6% after 200 cycles (Figure 2.12B). Additional testing was performed on the ZIF-8-500 electrode plating and stripping behavior using a fixed plating capacity of 1.0 mAh cm^{-2} and various current densities varying from 1.0 to 30.0 mA cm^{-2}. As seen in Figure 2.13, the ZIF-8-500 electrode shows extremely stable Coulombic efficiencies during 200 plating and stripping cycles at various applied current densities. The coulombic efficiency steadily increases to reach around 99.8% (98-200 cycles) at a high current density of 30.0 mA cm^{-2} (Figure 2.13), showing that the ZIF-8-500 electrode is promising for the development of a high-capacity zinc anode. Therefore, it can be concluded that the use of suitable temperature can enhance the withstand of high capacitance and high current density[12].

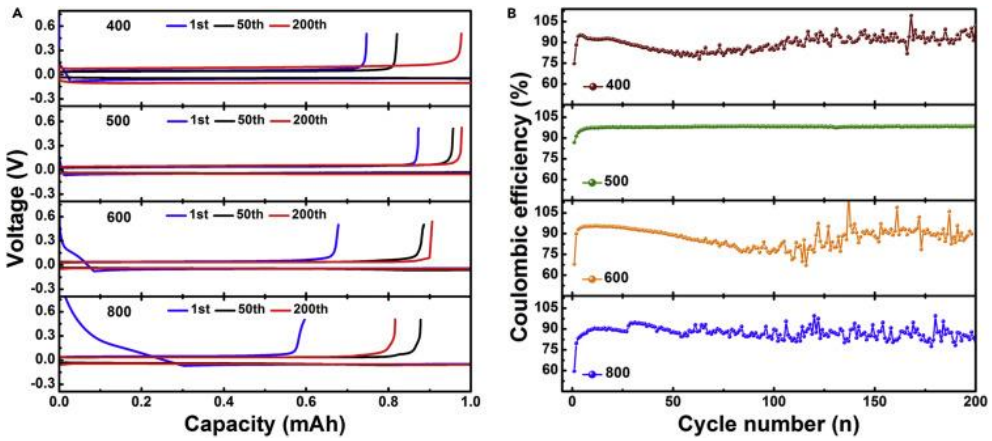

Figure 2.12 Electrochemical Performance of zinc Metal Anodes at a capacity of 1.0 mAh cm^{-2} and current density of 2.0 mA cm^{-2}. (a.) The galvanostatic plating and stripping curves (voltage versus capacity) at the selected cycles and (b.) the Coulombic efficiency over 200 cycles. [12]

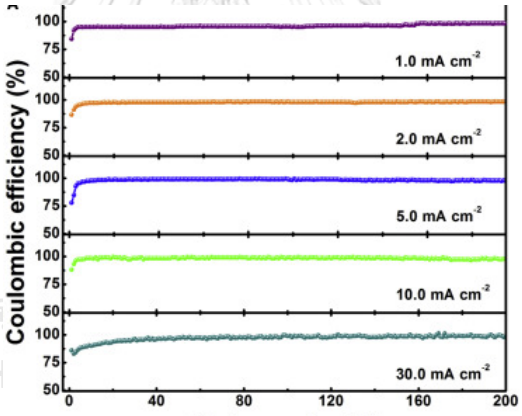

Figure 2.13 The zinc plating and stripping behavior of the ZIF-8-500 electrode was further tested capacity of 1.0 mAh cm^{-2} and various current densities varying from 1.0 to 30.0 mA cm^{-2}. [12]

Chapter III

Experiments

3.1 Materials

Zinc nitrate 98% ($Zn(NO_3)_2$) · H_2O was purchased from Ajax Finechem, polyvinylpyrrodidone $(C_6H_9NO)_n$ was purchased from Sigma-Aldrich, sodium hydroxide pellets (98%, AR) (NaOH) was purchased from LOBAChemie, 1,3,5-benzenetricarboxylic acid (>98%) ($C_6H_3(CO_2H)_3$) was purchased from TCI Chemicals, imidazole (99%) ($C_3H_4N_2$) was purchased from Alfa Aesar, ethyl alcohol (Grade AR) (99.9%) was purchased from QReC, n-methylpyrrolidone (AR grade) (NMP) was purchased from Quality reagent chemicals, poly (vinylidene fluoride) (Solef®PVDF) (MW. 180,000 g/mol) was purchased from Solvay, zinc sulfate 7 -hydrate ($(ZnSO_4) \cdot 7H_2O$) (AR grade, MW 287.58 g/mol) was purchased from Kemaus. Zinc foil (thickness: 0.1 mm), graphite foil (thickness: 0.05 mm), glass microfiber paper (GF/A, Whatman) and blank coin cell CR2025 were used as received.

3.2 Synthesis of Metal-Organic frameworks materials

MOFs were prepared according to a previously reported procedure [20].

Solution A: $Zn(NO_3)_2 \cdot H_2O$ 3.64 g and 0.25 g of polyvinyl pyrrolidone were dissolved in ethanol/ H_2O (62.5/62.5 mL)

Solution B: H_3BTC 5.625 mg, imidazole 1.82 g and NaOH 1 g were dissolved in ethanol/ H_2O (100/100 mL).

Then, solution B was dripped into solution A and stirring for 2 h, the mixture was transferred to a 100 mL Teflon-lined stainless-steel autoclave and then was placed in an oven for 20 h at a reaction temperature of 120 °C. Finally, it was washed several times with deionized water and ethanol and drying in an oven at

80°C overnight. The pyrolysis of metal-organic frameworks materials were prepared according to a previously reported procedure. [12]. The as-synthesized MOFs were subsequently thermally treated at different high temperatures (500°C, 600°C, 700°C, and 800°C, respectively) with a heating rate of 5°C/min under flowing N_2 for 3 h.

3.3 Preparation of CR2025 battery type

3.3.1 Anode preparation

3.3.1.1 Preparation of MOFs coated zinc foil (MOFs@Zn)

The MOFs was mixed with super-P and polyvinylidene fluoride (PVDF) in n - methylpyr rolidone (NMP) solution with the weight ratio of MOFs : Super-P : PVDF as a binder was 80 : 10 : 10, that was prepared under stirring at room temperature until homogeneous. It was then pressed onto a zinc foil (thickness, 100 μm) by the doctor blading method, the thickness of the MOFs coating layer was 160 μm., and dried at 80 °C for overnight in a vacuum oven to evaporate the solvent. The MOFs coated zinc foil was rolled with thickness 0.16 mm by battery roller machine.

3.3.2 Electrolyte preparation and separator preparation

The electrolyte in batteries was 2 M $ZnSO_4$, and the electrolyte preparation was to dissolve a certain amount of $ZnSO_4$ into DI water under stirring at room temperature until a homogeneous solution was achieved. The separator was a glass microfiber (pore size: 1.2 μm), which was cut into a circular shape with 19 mm in diameter.

3.3.3 Battery Assembly

The batteries were fabricated as a CR2025 coin cell that includes the top cap, spring, spacer, anode, separator, cathode, and bottom cap, respectively. The separator was soaked in 2 M $ZnSO_4$ electrolyte for 15 minutes while the component was being assembled. A crimping machine was then used to close the cell with a pressure of around 1 ton cm^{-2}.

3.4 Material Characterizations

3.4.1 Field emission scanning electron microscope (FE -SEM)

The MOFs samples as a powder (MOFs, MOFs-500°C, MOFs-600°C, MOFs-700°C, and MOFs-800°C) were examined by the field emission scanning electron microscope (FE-SEM) to visualize very small morphology details on the surface of sample as expanding to 5 μm and expanding up to 50 μm providing an in-depth detail of the MOFs.

3.4.2 Energy-dispersive X-ray spectroscopy (EDS)

Energy-dispersive X-ray spectroscopy (EDS) is a type of scanning electron microscopy that examined by X-rays to identify the elemental composition of the MOFs samples (MOFs, MOFs-500°C, MOFs-600°C, MOFs-700°C, and MOFs-800°C). The EDS mapping analysis is used to determine the composition of the elements of MOFs such as N, Zn, C, and O and expanding up to 50 μm providing an in-depth detail of the MOFs.

3.4.3 Surface area and porosity analysis (BET)

The MOFs samples (MOFs, MOFs-500°C, MOFs-600°C, MOFs-700°C, and MOFs-800°C) were determined by Brunauer-Emmett-Teller (BET) to identify the specific surface area.

3.4.4 X-Ray Diffractometer (XRD)

The MOFs powder samples (MOFs, MOFs-500°C, MOFs-600°C, MOFs-700°C, and MOFs-800°C) were examined by X-Ray Diffractometer (XRD) to analyze physical properties.

3.4.5 X-ray Absorption Spectroscopy (XAS)

X-ray Absorption Spectroscopy (XAS) is a used technique for determining the local geometric and/or electronic structure of matter. The experiment is usually performed at synchrotron radiation facilities, which provide intense and tunable X-ray

beams. The MOFs samples (MOFs, MOFs-500°C, MOFs-600°C, MOFs-700°C, and MOFs-800°C) were examined by the X-ray absorption spectroscopy (XAS) spectra of the Zn k-edge for 4 times to provide important information about the structure and chemical bonding of the zinc phase.

3.5 Electrochemical measurements

3.5.1 Galvanostatic charge/discharge cycling

The galvanostatic cycling test was the standard by measuring the striping/plating performance of bare Zn||bare Zn, MOFs@Zn||MOFs@Zn, and MOFs-X@Zn||MOFs-X@Zn (which X = 500°C, 600°C, 700°C, 800°C) in symmetrical cells, the galvanostatic cycling test was the standard method for determining the cell performance. The long-term cycling performance and cycling stability of the zinc anodes were evaluated at a current density of 1, 2 and 3 mA $cm^{-2}$with fixed capacity of 1 mAh cm^{-2}. Battery tester was utilized to test this method.

3.5.2 The Coulombic efficiency (CE)

The coulombic efficiency (CE), used to assess the battery's reversibility, was the ratio of discharging capacity to charging capacity. At a current density of 1 mA $cm^{-2}$with a fixed capacity of 1 mAh cm^{-2}, the CE of bare and coated copper (bare Cu||bare Zn, and MOFs-500°C@Cu||bare Zn) was measured.

$$\text{Coulombic efficiency} = \frac{\text{Discharging capacity}}{\text{Charging capacity}} \times 100\% \qquad \text{(eq.3.1)}$$

3.5.3 Electrochemical impedance spectroscopy (EIS)

EIS measurements were carried out with VersaSTAT tool over the frequency range between 100,000 Hz and 0. 1 Hz with an AC voltage of 10 mV. This test was conducted via the potentiometer on coin cell including bare and coated (bare Zn,

MOFs@Zn, MOFs-500°C@Zn, MOFs-600°C@Zn, MOFs-700°C@Zn, and MOFs-800°C@Zn which were the working electrode, zinc foil was counter and reference electrode. The batteries before cycling were observed. The result showed impedance spectra that indicated the electronic and ionic conductivities.

Chapter IV

Result and discussion

4.1 The characterization of zinc anode

The MOFs synthesized by hydrothermal method is white powder as shown in Figure A1 A, and when pyrolyzed, it changes from white to brown to black at high temperatures because MOFs was change to carbon as shown in Figure A1 B-E. The FESEM images reveal the morphology of MOFs, which displays a unique shape resembling a square bar with a pointy end as shown in Figure 4.1 as expanding to 5 μm and expanding up to 50 μm providing an in-depth detail of the MOFs. The components from the EDS mapping analysis are shown in Figure 4.1 as Zn in red, C in pink, N in yellow, and O in green. These substances are derived from the -COOH ligands of 1,3,5-benzene tricarboxylic acid and N-ligand from Imidazole. Wu [26] reported newly synthesized MOFs using Zn as the metal and two ligands, Imidazole, and BTC. The structure is shown in Figure 4.2. the synthesis method and substance of this work are similar to those of our work, so it is assumed that the Zn-BTC-Imidazole (MOFs) structure of our work is similar to that of Figure 4.2. [26]

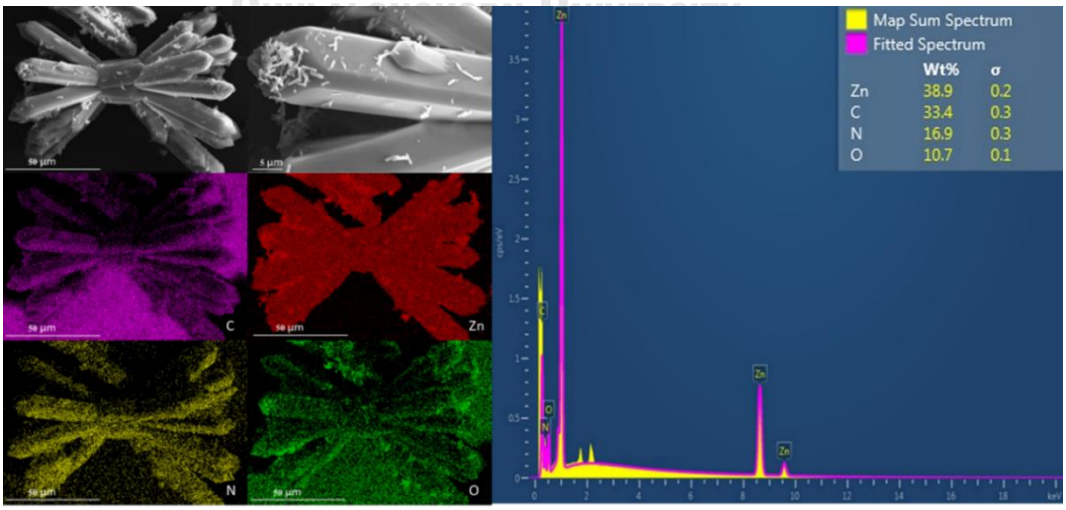

Figure 4.1 FESEM image of Zn-BTC-Imidazole (MOFs)

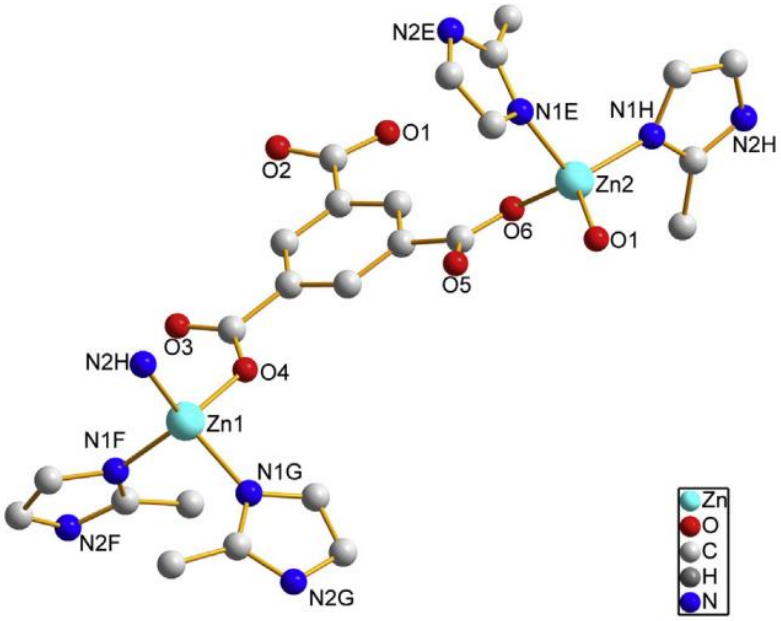

Figure 4.2 Possible structure of Zn-BTC-Imidazole (MOFs) [26]

Fourier-transform infrared spectroscopy (FTIR) as shown in Figure 4.3 is used to confirm the synthesized functional group of Zn-BTC-imidazole (MOFs). The primary functional group of the produced MOFs, Zn-O, is the functional group of the BTC ligand, while the main functional group of Zn-N is the functional group of the imidazole ligand. The stretching vibrations of O-H groups associated with physically bound water molecules were the primary cause of the large adsorption band at 3500–3000 cm^{-1}. When the main functional groups of the ligands utilized are Zn-O and Zn-N, bands in the 800-600 cm^{-1} region are generated. [27, 28] From figure 4.3, FTIR pattern of MOFs and MOFs-500°C are similar. When pyrolyzed at 500°C, the functional group of MOFs-500°C can be retained. However, when pyrolyzed at 600°C, 700°C, and 800°C, FTIR pattern were quite different when compare with MOFs, because the structure of the MOFs were decomposed, and the functional group disappeared when pyrolyzed at high temperature.

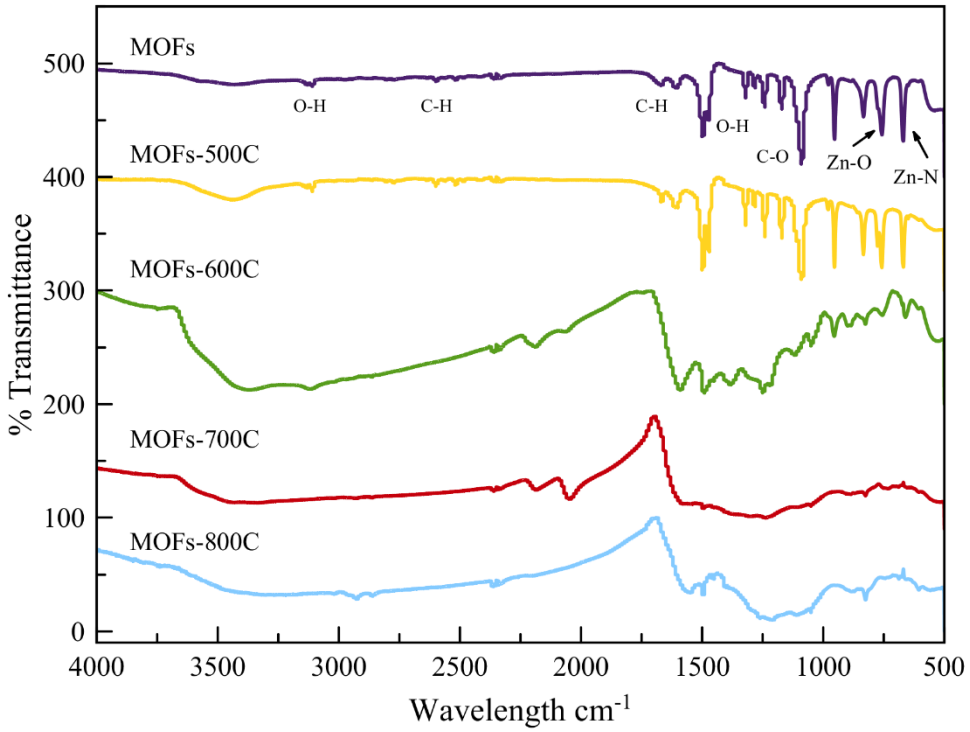

Figure 4.3 FTIR of Zn-BTC-Imidazole (MOFs, MOFs-500℃, MOFs-600℃, MOFs-700℃, and MOFs-800℃)

XRD analysis is used to confirm the phase purity of the as-synthesized MOFs. Figure 4.4 shows that the diffraction pattern of the as-synthesized MOFs is identical to the patterns. Figure. 4.4A shows that the comparison of MOFs and substrate XRD pattern, which results in the MOFs identity peak not matching with the substrate identity peak because the new crystal structure has already been formed. Wu et al. has synthesized MOFs using Zn as metal and Imidazole and BTC are ligands, which are very similar to our work. We took the XRD peak of Wu as the reference peak for our work to ensure that we successfully synthesized MOFs (Zn-BTC-Imidazole). The XRD of Zn-BTC-Imidazole (MOFs) was compared with Wu's work (Reference XRD) as shown in Figure A2 [26]. The reference XRD uses zinc as the metal and its ligands are imidazole and BTC, which are similar to our work and have main peaks at the same peak. This indicates that the crystal materials have been successfully reconstituted. The MOFs materials have zinc linked to the N atoms of imidazole and are also

coordinated by BTC via Zn-O bonds. Then, when pyrolyzed as shown in Figure 4.4B, it was found that XRD showed that at 500°C the graph was still intact, and there was a peak that was very close to MOFs, but if pyrolyzed at a temperature higher than 500°C, it was found that the peak of FTIR and XRD significantly changed as a result of the decomposition of the MOFs structure and turn into amorphous carbon, which is an unstable phase. [12, 29].

The X-ray absorption spectroscopy (XAS) spectra of the Zn k-edge provide important information about the structure and chemical bonding of the zinc phase. The samples are pyrolyzed as shown in Figure 4.5. When compared to Zn-BTC-Imidazole (MOFs) and the reference curves of Zn-N and Zn-O [30], which occur at 1-2 Å ref, Zn-BTC-Imidazole (MOFs) has the largest base because of the combination of the Zn-N and Zn-O curve. The Zn bonding to the ligand disappears during pyrolysis at temperatures above 500°C, which results in a partial disappearance of the Zn-O and Zn-N structures and a decrease in the MOFs-500°C -800°C curve. The addition of raising the pyrolysis temperature from 600°C to 800°C causes Zn-N and Zn-O to decompose, which causes the base of the graph to narrow.

The pore size of the MOFs and MOFs-X can be tested by using surface area and porosity analysis (BET). The pore size of the MOFs that can make zinc-ions pass well must be neither too small nor too large (2 nm) [31], From the experimental results, it was found that MOFs and MOFs-500°C have a radius that allows zinc-ions to pass easily around 13 Å and 15 Å, but the MOFs that pyrolyze at 600-800°C have the radius around 5-9 Å (Figure 4.6), which is too small, it unlikely that zinc-ions will be able to pass through, thus possibly reducing the electrical effect.

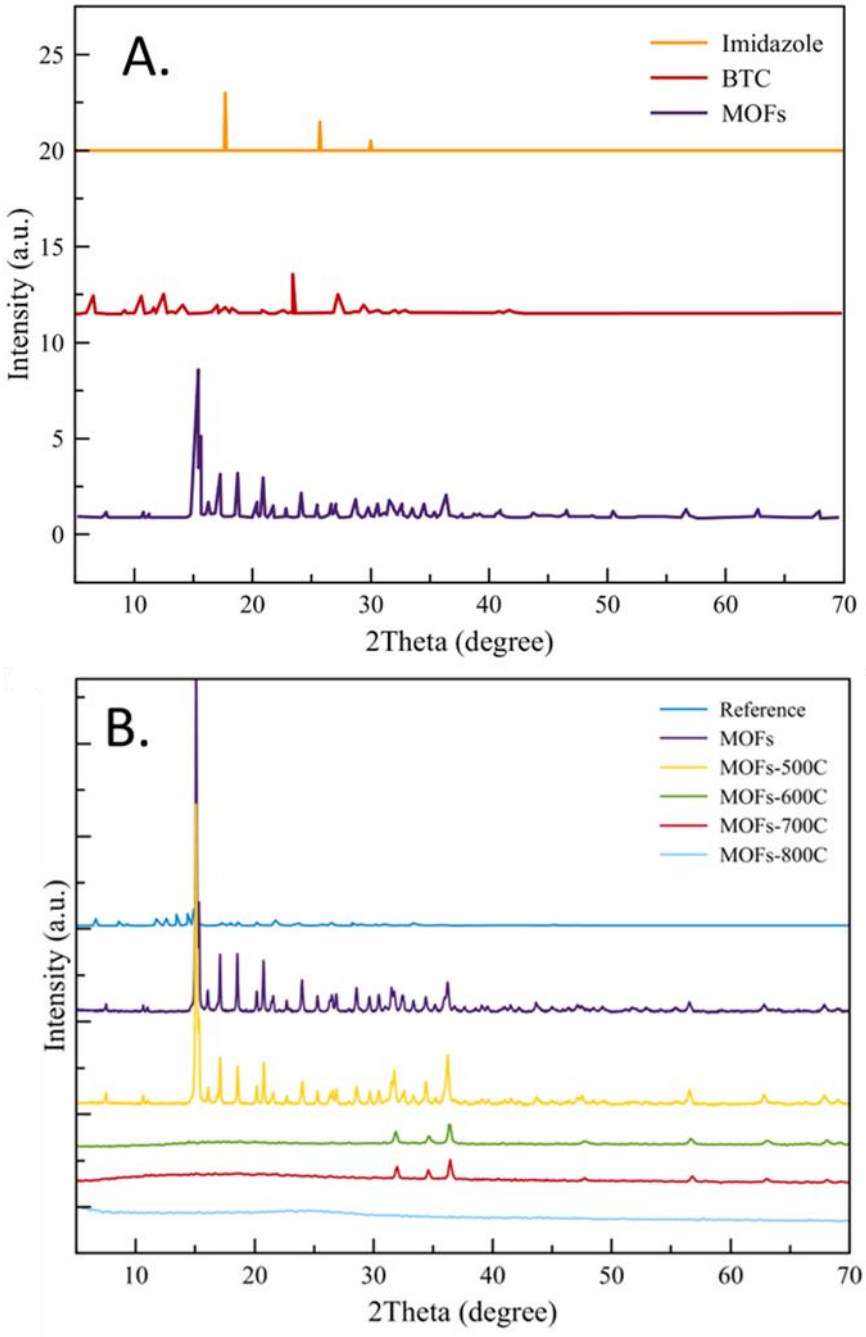

Figure 4.4 XRD pattern of Zn-BTC-Imidazole (A.) Zn-BTC-Imidazole compared with reference (B.) Zn-BTC-Imidazole compared with MOFs, MOFs-500°C, MOFs-600°C, MOFs-700°C, and MOFs-800°C

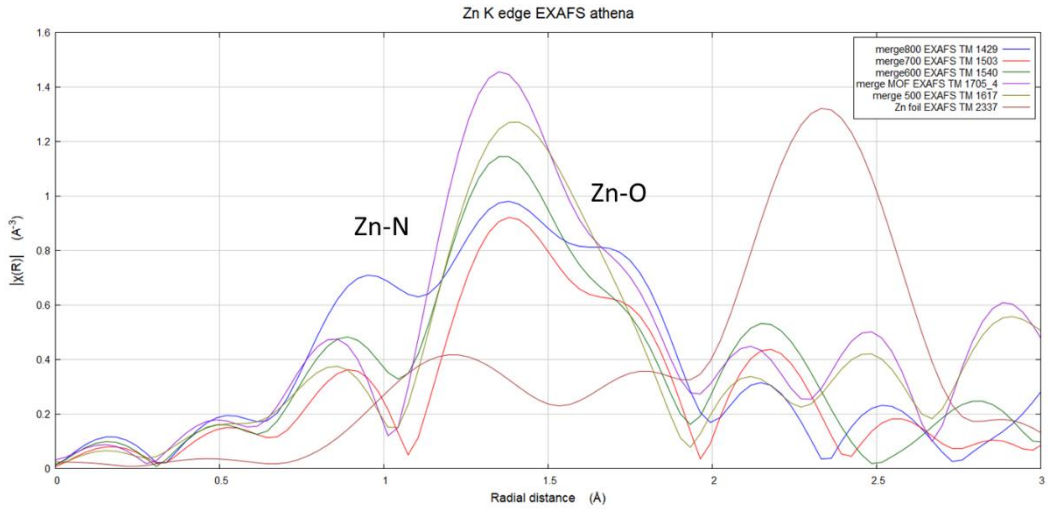

4.5 XAS (Zn K-edge EXAFS) pattern of Zn-BTC-Imidazole (MOFs, MOFs-500°C, MOFs-600°C, MOFs-700°C, and MOFs-800°C)

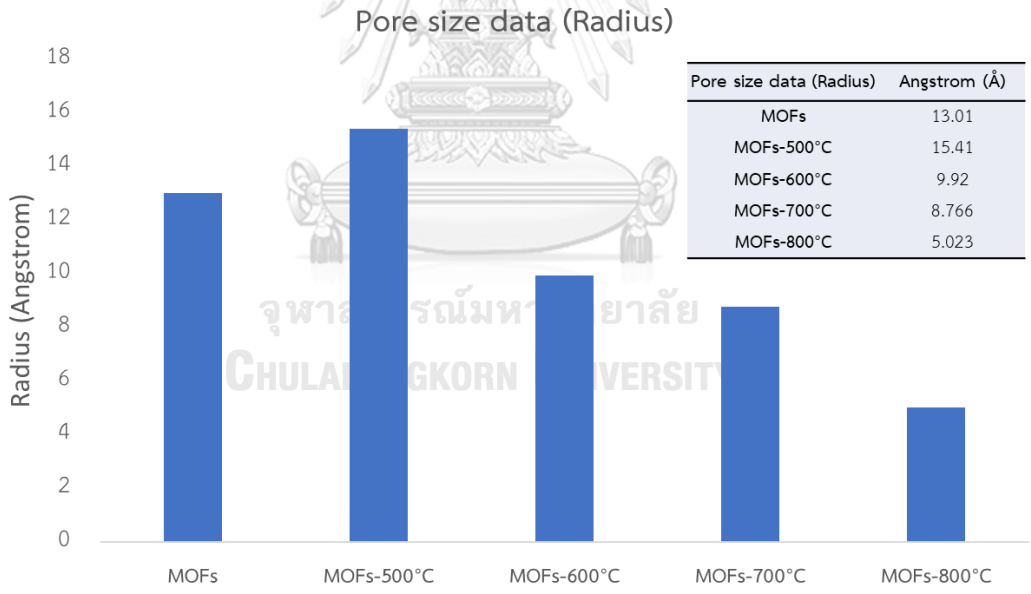

Pore size data (Radius)	Angstrom (Å)
MOFs	13.01
MOFs-500°C	15.41
MOFs-600°C	9.92
MOFs-700°C	8.766
MOFs-800°C	5.023

Figure 4.6 Pore size data from BET analysis of MOFs, MOFs-500°C, MOFs-600°C, MOFs-700°C, and MOFs-800°C Figure

Figure 4.7, Showed the appearanceafter the bare Zn and coated zinc foils by MOFs-X were soaked in 2 M $ZnSO_4$ electrolyte, After several days of soaking, there was found that the coated zinc by MOFs hardly changed, while the bare Zn was

corroded and turned into a dark gray and rust-yellow color. The MOFs-X coating effectively reduced the electrolyte corrosion of the zinc anode due to the absence of by-products. The coating layer, composed of MOFs-X and PVDF binder, acted as an artificial SEI layer, preventing direct contact between the anode and the electrolyte and reducing the generation of by-products. These results demonstrate the potential of the MOFs-X coating as a promising material for improving the corrosion resistance and overall performance of zinc-ions batteries.

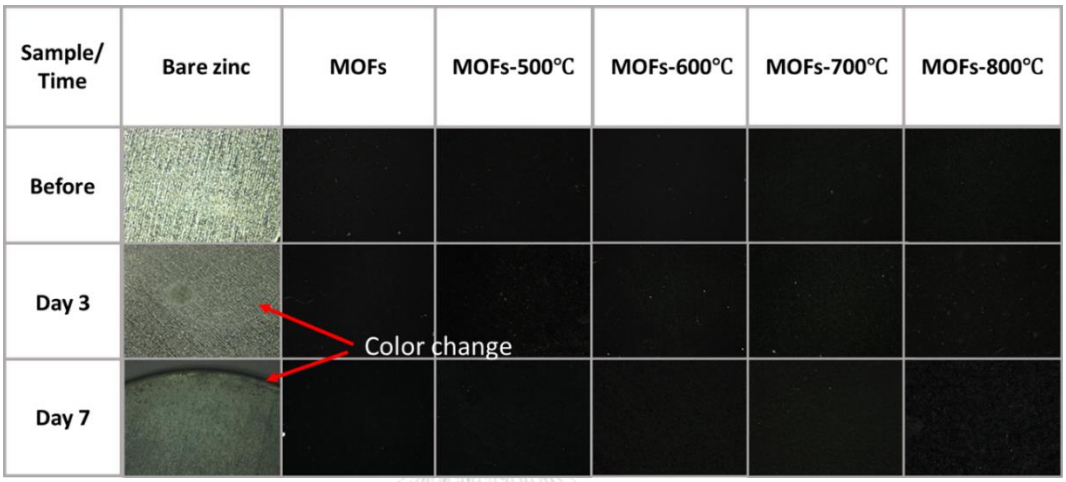

Figure 4.7 Photographs of bare Zn and coated Zn soaked in a 2 M $ZnSO_4$ electrolyte.

4.2 Impedance and ionic conductivity of zinc anode

The study aimed to examine the impedance and ionic conductivity of zinc electrodes with different coatings in concentrated aqueous electrolyte of 2 M $ZnSO_4$. The electrodes tested included bare Zn, MOFs@Zn, MOFs-500°C @Zn, MOFs-600°C @Zn, MOFs-700°C @Zn, and MOFs-800°C @Zn. The results showed that the MOFs-X interfacial coating layer (MOFs@Zn, MOFs-500°C @Zn, MOFs-600°C @Zn, MOFs-700°C @Zn, and MOFs-800°C @Zn) significantly lowered the impedance of the zinc anode compared to the bare Zn. The impedance spectra of the bare zinc showed a higher impedance than zinc coated with MOFs-X. According to the findings, the MOFs-X coating layer greatly decreased the resistance of charge transfer at the electrode interface and the transport of zinc-ions through the SEI layer of the anode. The presence of MOFs can control Zn^{2+} flux, decrease excessive nucleation, and limit

side reactions. This finding suggests that the MOFs-X coating layer improves zinc-ions transport and charge transfer to improve the zinc anode's overall performance. In addition to layered MOFs, the SEI layer can reduce the problem of electrolyte corrosion. MOFs contain a perfectly specific porous morphology and fully active sites that serve as routes for zinc-ion transfer, as well as various molecular topologies that improve electrochemical performance[32]. The presence of a lattice-like MOFs additionally allows fast and orderly migration of the passing zinc-ions. The zinc-ions passing through MOFs are organized by their lattice-like structure, which prevents them from concentrating in one area. Additionally, the MOFs contains a metal (Zn) structure that functions as a stationary phase [33], where the metal is located in the center and strongly binds to the ligand. The N ligand and the N-doped carbon from pyrolysis can attract the zinc-ions similar to the zinccophelic site, which attracts zinc-ions like a magnet to allow zinc-ions to pass through easily and quickly. These contribute to lower system resistance as they reduce charge transfer resistance.

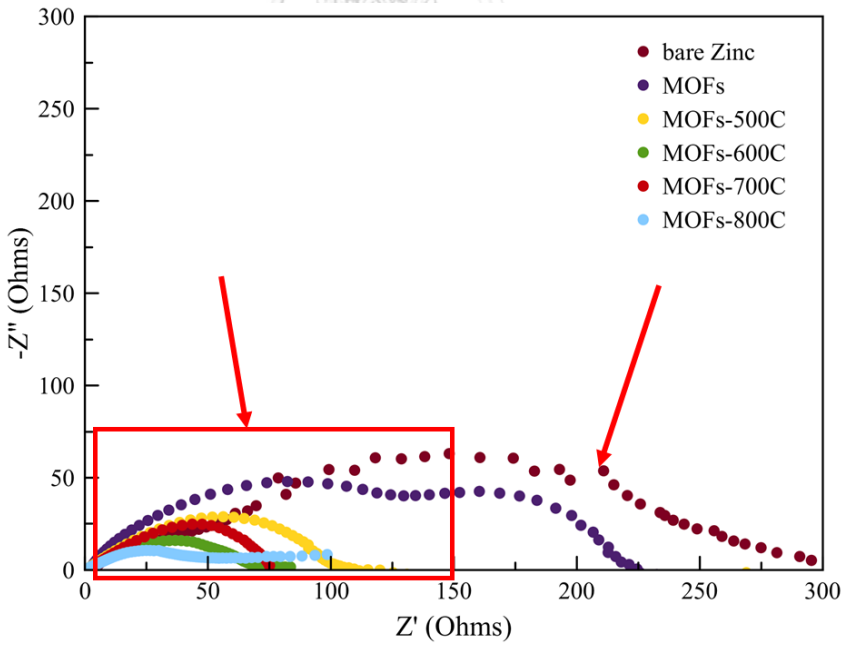

Figure 4.8 Electrochemical impedance spectra (EIS) of symmetric cells with bare Zn, MOFs, MOFs-500℃, MOFs-600℃, MOFs-700℃, and MOFs-800℃.

4.3 Galvanostatic charge/discharge cycling

The stability of symmetrical zinc cells was evaluated using bare Zn and MOFs-X@Zn at various temperatures of pyrolysis and combined 2 M $ZnSO_4$ electrolyte. The galvanostatic cycling test was performed at various current densities of 1, 2 and 3 mA cm^{-2} with a fixed capacity of 1 mAh cm^{-2}, as shown in Figure. 4.9. The cycling curves of bare Zn cells exhibit extreme vibrations and short circuits (around 35 h). Due to dendrites, corrosion, and hydrogen bubbles that were seen on the surface of bare Zn during the charge/discharge process of ZIBs, there is an uneven current distribution [6, 7, 9, 10, 34]. The cycling curve of MOFs-X@Zn, meanwhile, is more stable than that of bare Zn, The results from Figure 4.9A demonstrate that MOFs-500°C@Zn has a significantly longer battery life of more than 600 hours at a current density of 1 mAh cm^{-2}, compared to MOFs-600°C@Zn, MOFs-700°C@Zn, and MOFs-800°C@Zn, which exhibit extreme vibrations and short-circuits after less than 200 hours of cycling. The MOFs-500°C@Zn has shown a greater ability to cycle at high currents than the other samples, with a cycling time of over 400 hours, when the current density is increased to 3 mA cm^{-2}. This improved stability is attributed to the presence of imidazole and BTC ligands, that can coordinate with Zn2+, resulting in homogenous Zn deposition on the anode surface and the carboxyl groups and N atoms in the organic ligands provide them with more complicated and varied coordination modes. Between the aromatic rings, there are additional H-bond and "**π**" – "**π**" stacking effects, which can considerably improve conductivity by promoting electron delocalization and dispersion, resulting in a decrease in zinc anode development[24, 25]. The FTIR and XRD analysis can confirm the presence of the ligand. The main functional groups of MOFs are still obvious in XRD and FTIR graphs, which have a substantial impact on long-life performance of batteries. Additionally, the pyrolysis of MOFs creates graphene oxide phase [35] and porosity that is more zinc-like, performing as a zincophilic sites for zinc-ions and allowing them to move through easily and in an orderly manner [36]. This makes the MOFs-500°C@Zn more stable and enables it to handle high currents for extended periods of cycle time. At high temperatures from MOFs-600°C@Zn, MOFs-700°C@Zn, and

MOFs-800°C@Zn, undesirable phase carbon synthesis and oxidation can occur, which may cause the creation of dendrites or other side reactions in MOFs. The XRD and FTIR pattern of MOFs-600°C@Zn, MOFs-700°C@Zn, and MOFs-800°C@Zn, have a significant change in the graph compared to MOFs pattern. At high temperature, the imidazole ligand and BTC ligand functional group have already decomposed and turned into amorphous carbon, resulting in a shorter battery life compared to MOFs-500°C@Zn. Moreover, pyrolysis at temperatures below 500°C causes uneven distribution of Zn(0), so it is not used in batteries [12].

The battery life cycle of MOFs-600°C@ Zn, MOFs-700°C@ Zn, and MOFs-800°C @Zn cannot be tolerated at high current densities, and the cycle time is short. The stability and overall performance of the anode may suffer as a result. According to the findings from Figure 4.9, MOFs-500°C @Zn is a better sample for battery applications because it has a longer battery life and better performance at high current densities. The MOFs layer acts as an SEI layer that ensures the surface of the anode remains smooth and maintains a uniform morphology even when zinc-ions are obtained at a high area capacitance. This layer helps to eliminate the formation of dendrites, which can degrade the performance of the anode. The porous carbons in the anode retain a significant amount of oxygen functionality in the form of COOH, which along with the N, provide sites for zinc-ions to reside and move readily in the porous carbon structure. This enhances the stability of the anode and ensures that it can withstand high current density. Overall, the combination of the MOFs layer and the porous carbon in the anode provides a stable and efficient platform for zinc-ion battery applications.

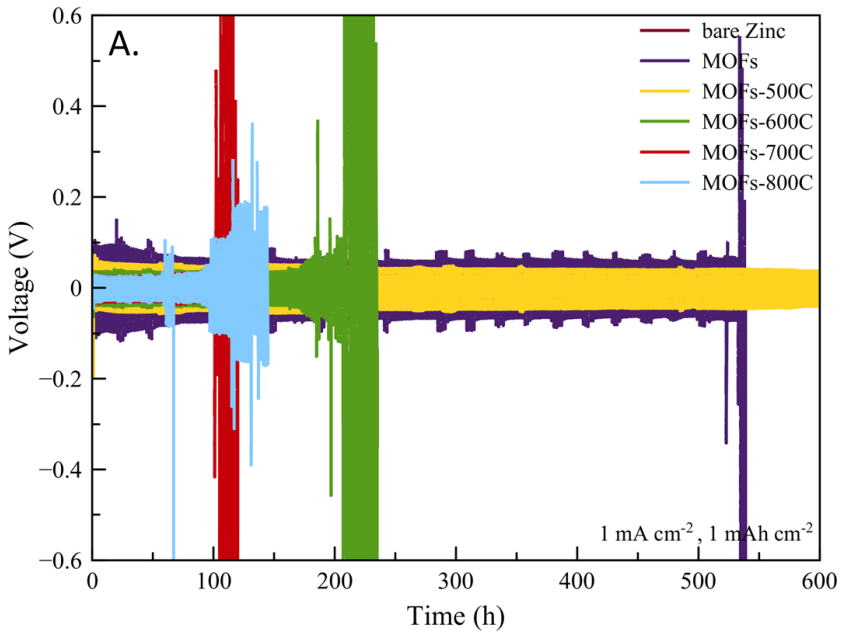
A.
bare Zinc
MOFs
MOFs-500C
MOFs-600C
MOFs-700C
MOFs-800C
1 mA cm-2 , 1 mAh cm-2
Voltage (V)
Time (h)
0.6
0.4
0.2
0
−0.2
−0.4
−0.6
0
100
200
300
400
500
600

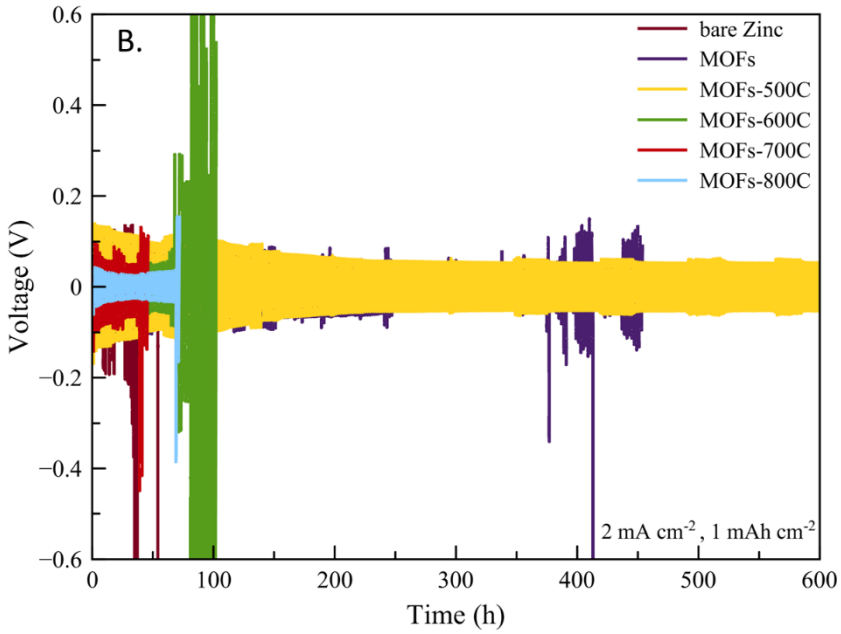
B.
bare Zinc
MOFs
MOFs-500C
MOFs-600C
MOFs-700C
MOFs-800C
2 mA cm-2 , 1 mAh cm-2
Voltage (V)
Time (h)
0.6
0.4
0.2
0
−0.2
−0.4
−0.6
0
100
200
300
400
500
600

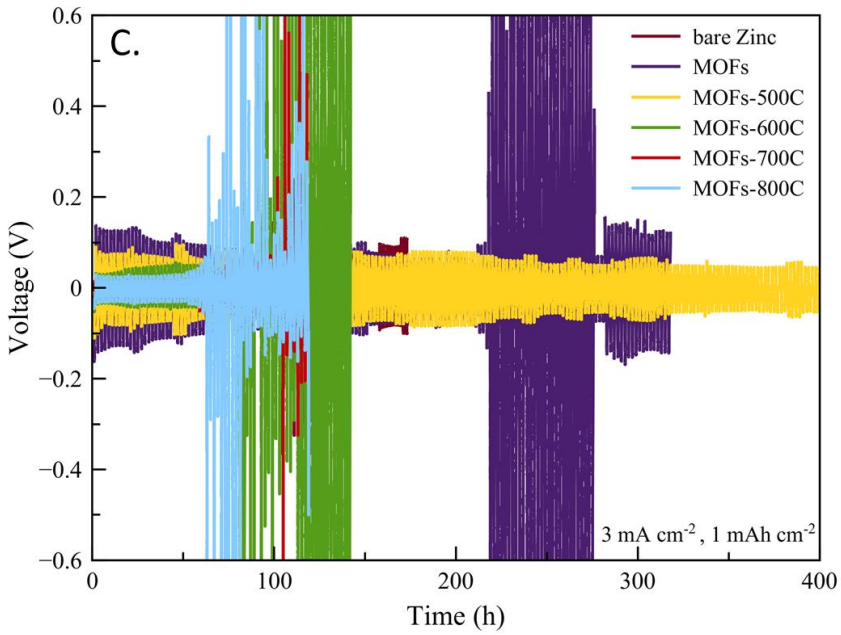

Figure 4.9 The cycling performance of symmetrical zinc cells with bare Zn and MOFs-X@Zn at various temperature of pyrolysis. (A.) At a current density of 1 mA $cm^{-2}$and capacity of 1 mAh cm^{-2}. (B.) At a current density of 2 mA $cm^{-2}$and capacity of 1 mAh cm^{-2}. (C.) At a current density of 3 mA $cm^{-2}$and capacity of 1 mAh cm^{-2}.

4.4 The Coulombic efficiency (CE)

The purpose of the experiment was to investigate the effect of the MOFs-500℃ coating layer on the coulombic efficiency (CE) of the reversibility of the Zn/Zn^{2+} process. In each cycle, zinc was dissolved from the zinc metal as a cathode and deposited onto the copper as an anode. To study the CE, a MOFs-500℃ coating layer was coated on copper foil (MOFs-500℃@Cu) and then tested half cells (MOFs-500℃@Cu||bare Zn) compared with bare Cu||bare Zn.

The test was carried out by plating zinc (fixe) areal capacity: 1 mAh cm^{-2}) onto the MOFs-500℃@Cu and Cu substrate and then stripping to -0.4 V. As shown in Figure 4.10, the bare Cu electrode exhibited fluctuant voltage signals during zinc plating/stripping due to side reactions such as dendrite formation, hydrogen

evolution reaction (HER), and corrosion. In contrast, the MOFs-500°C@Cu cell presented a very stable coulombic efficiency (CE) over 50 cycles (100 h), maintaining an average CE of 98.42%.

This suggests that the MOFs-500°C coating layer can significantly improve the stability and efficiency of zinc-ions batteries by preventing undesirable side reactions and dendrite formation during cycling. These results demonstrate the potential of MOFs-500°C as a promising coating material for improving the performance and durability of zinc-ions batteries.

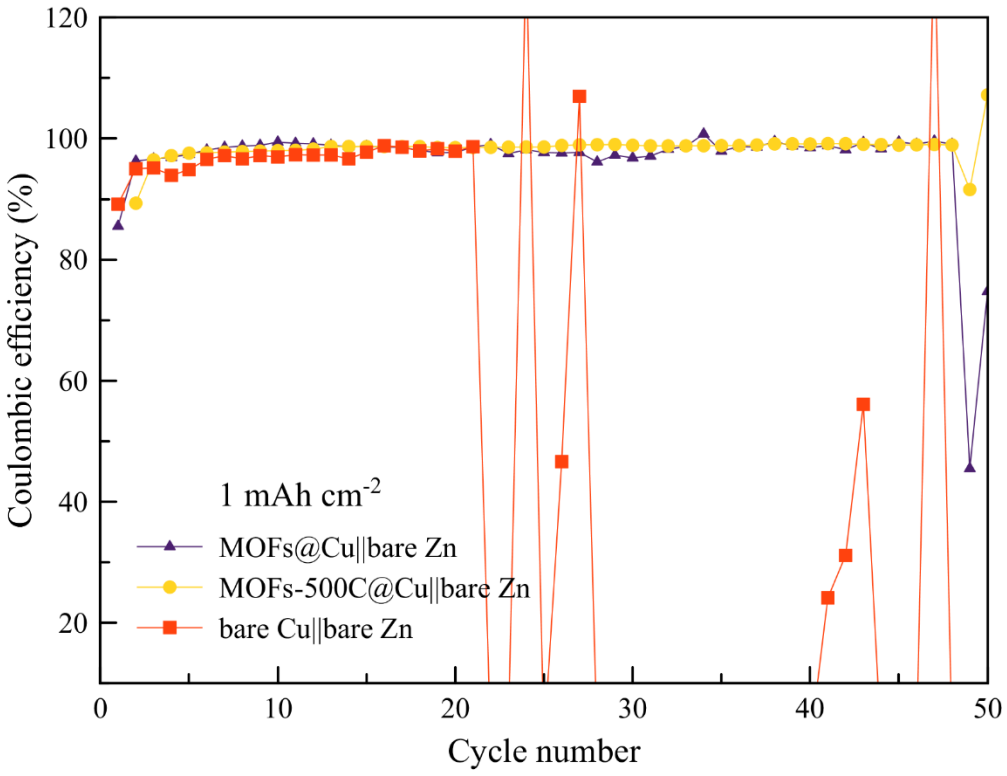

Figure 4.10 The coulombic efficiency (CE) of zinc plating/stripping in the bare Cu||bare Zn, MOFs°C@Cu||bare Zn and MOFs-500°C@Cu||bare Zn half cells.

Chapter V

Conclusion

In this work, MOFs was newly synthesized as dual MOFs ligands with metal as zinc and BTC and imidazole as ligands, after which pyrolysis was performed to add carbon atoms and zinc atoms to the porosity of MOFs at MOFs-X (MOFs-500℃, MOFs-600℃, MOFs-700℃, and MOFs-800℃). The MOFs was coated to zinc anode as the SEI layer and their performance was compared with the bare zinc. The corrosion test by soaking MOFs-coated zinc anodes and bare zinc in 2M $ZnSO_4$ showed that the MOFs-coated anodes prevented the anodes and almost no change in corrosion, but bare zinc has turned dark gray after 3-7 days of soaking in the electrolyte. To test the impedance and ionic conductivity of zinc electrodes with bare zinc and MOFs-X, the impedance of the zinc anode was lowered by MOFs and MOFs-X more than by bare zinc in the Nyquist curves of impedance spectra of the various anodes. Results indicated that the maximum ionic conductivity was found in MOFs@Zn and MOFs-500@Zn, which indicated that Zn^{2+} moved rapidly through the MOFs layer. Table 2 shows the result on electrochemistry performance with different methods for modifying zinc anodes. From the long-term cycle battery test of Zn-BTC-Imidazole (MOFs-500℃, MOFs-600℃, MOFs-700℃) it was found that The MOFs-500℃ has the longer battery life and can resist high current densities than other works because of the internal structure of the MOFs. Pyrolysis produces a good electrically conductive carbon atom and a zincophilic sites attract zinc-ions to pass through in an orderly manner, which can reduce the problem of dendrite formation by pyrolysis. The zinc-ions move repeatedly and ultimately cause the battery to short circuit. Due to the presence of layered MOFs as SEI layer can control the zinc-ions distribution and uniform nucleation position for zinc deposition on the anode surface and adding

the MOFs layer as the SEI layer to prevent the zinc anode from attaching directly to the separator and prevent corrosion from electrolyte. The cycling stability can be as high as 600 hours. Coated with MOFs, it is interesting to study and develop full-cell battery for rechargeable aqueous zinc-ion batteries with high cycle stability and long battery life as well as environmental friendliness in the future.

Appendix

Table 2 Different methods for modifying zinc anodes and their result on electrochemistry performance.

No.	System	Anode	Current density ($mA\ cm^{-2}$)	Capacity ($mAh\ cm^{-2}$)	Electrolyte	Worked time	References
1	ZIBs	ZIF-8-500C	1	1	2M $ZnSO_4$	400	[12]
2	ZIBs	ZIF-8	0.25	0.05	2M $ZnSO_4$	180	[13]
3	ZIBs	Zn-BTC	3	0.5	2M $ZnSO_4$	400	[19]
4	LIBs	ZIF-8 derived N/O	2	1	2M $ZnSO_4$+ H_2O	200	[37] Appendix
5	ZIBs	Zn-BTC-Imidazole MOFs-500°C	1	1	2M $ZnSO_4$	Over 600	This work
			3	1		Over400	

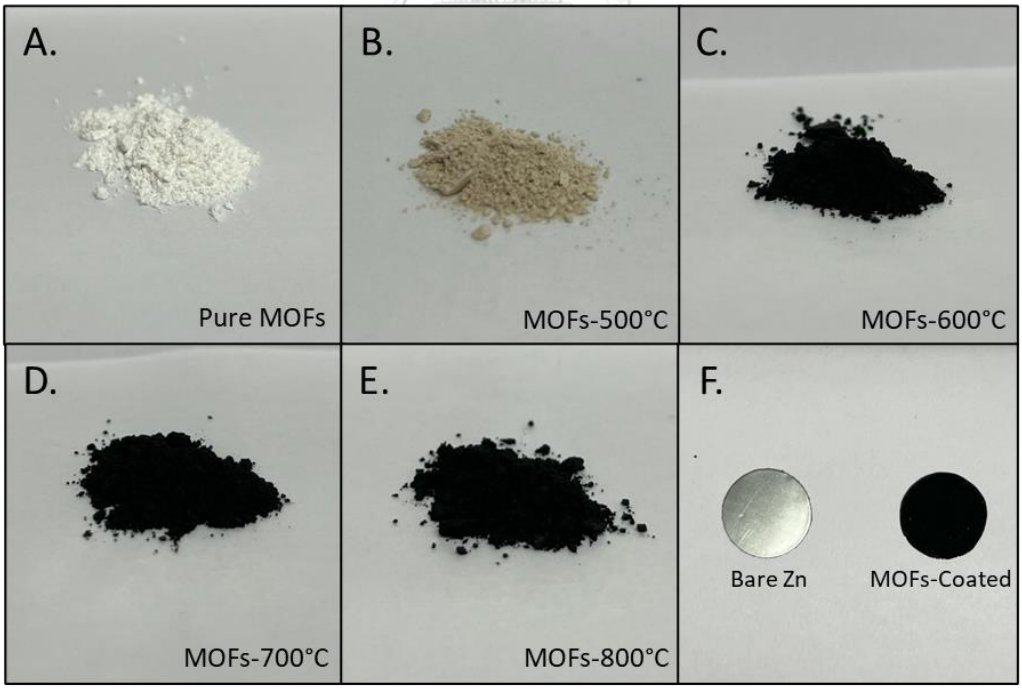

Figure A1 The MOFs samples powder (A.) Pure MOFS (B.) MOFs-500°C (C.) MOFs-600°C (D.) MOFs-700°C (E.) MOFs-800°C (F.) bare Zn and MOFs-coated anode electrode

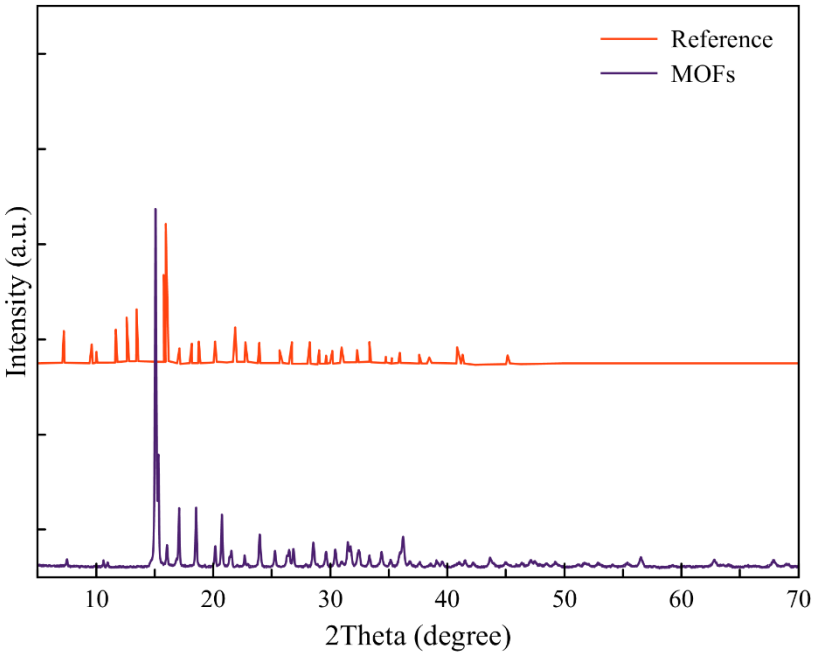

Figure A2 The XRD pattern of MOFs compared with reference work

REFERENCES

1. Bruce Dunn, Haresh Kamath, and Jean-Marie Tarascon, *Electrical Energy Storage for the Grid: A Battery of Choices.* Science, 2011. 334(6058): p. 928-935.
2. Naoki Nitta, Feixiang Wu, Jung Tae Lee, and Gleb Yushin, *Li-ion battery materials: present and future.* Materials today, 2015. 18(5): p. 252-264.
3. Daniel H Doughty and E Peter Roth, *A general discussion of Li ion battery safety.* The Electrochemical Society Interface, 2012. 21(2): p. 37.
4. Chengjun Xu, Baohua Li, Hongda Du, and Feiyu Kang, *Energetic zinc ion chemistry: the rechargeable zinc ion battery.* Angewandte Chemie, 2012. 124(4): p. 957-959.
5. Zhaowei Guo, Yuanyuan Ma, Xiaoli Dong, Jianhang Huang, Yonggang Wang, and Yongyao Xia, *An environmentally friendly and flexible aqueous zinc battery using an organic cathode.* Angewandte Chemie, 2018. 130(36): p. 11911-11915.
6. Y Zuo, K Wang, P Pei, M Wei, X Liu, Y Xiao, and P Zhang, *Zinc dendrite growth and inhibition strategies.* Materials Today Energy, 2021. 20: p. 100692.
7. Xin Zhang, Jun-Ping Hu, Na Fu, Wei-Bin Zhou, Bin Liu, Qi Deng, and Xiong-Wei Wu, *Comprehensive review on zinc-ion battery anode: Challenges and strategies.* InfoMat, 2022. 4(7): p. 1-28.
8. Shougo Higashi, Seok Woo Lee, Jang Soo Lee, Kensuke Takechi, and Yi Cui, *Avoiding short circuits from zinc metal dendrites in anode by backside-plating configuration.* Nature communications, 2016. 7(1): p. 1-6.
9. Aruuhan Bayaguud, Yanpeng Fu, and Changbao Zhu, *Interfacial parasitic reactions of zinc anodes in zinc ion batteries: underestimated corrosion and hydrogen evolution reactions and their suppression strategies.* Journal of Energy Chemistry, 2022. 64(1): p. 246-262.
10. Qi-Long Zhu and Qiang Xu, *Metal–organic framework composites.* Chemical Society Reviews, 2014. 43(16): p. 5468-5512.
11. Kranthi Kumar Gangu, Suresh Maddila, Saratchandra Babu Mukkamala, and Sreekantha B Jonnalagadda, *A review on contemporary metal–organic*

framework materials. Inorganica Chimica Acta, 2016. 446(1): p. 61-74.

12. Zhuo Wang, Jianhang Huang, Zhaowei Guo, Xiaoli Dong, Yao Liu, Yonggang Wang, and Yongyao Xia, *A metal-organic framework host for highly reversible dendrite-free zinc metal anodes.* Joule, 2019. 3(5): p. 1289-1300.
13. Xuechao Pu, Baozheng Jiang, Xianli Wang, Wenbao Liu, Liubing Dong, Feiyu Kang, and Chengjun Xu, *High-performance aqueous zinc-ion batteries realized by MOF materials.* Nano-micro letters, 2020. 12(1): p. 1-15.
14. Joakim Ekspong, Eduardo Gracia-Espino, and Thomas Wågberg, *Hydrogen Evolution Reaction Activity of Heterogeneous Materials: A Theoretical Model.* The Journal of Physical Chemistry C, 2020. 124(38): p. 20911-20921.
15. J. Shin, J. Lee, Y. Park, and J. W. Choi, *Aqueous zinc ion batteries: focus on zinc metal anodes.* Chem Sci, 2020. 11(8): p. 2028-2044.
16. T. Wang, C. Li, X. Xie, B. Lu, Z. He, S. Liang, and J. Zhou, *Anode Materials for Aqueous Zinc Ion Batteries: Mechanisms, Properties, and Perspectives.* American Chemical Society Nano, 2020. 14(12): p. 16321-16347.
17. Kangning Zhao, Chenxu Wang, Yanhao Yu, Mengyu Yan, Qiulong Wei, Pan He, Yifan Dong, Ziyi Zhang, Xudong Wang, and Liqiang Mai, *Ultrathin Surface Coating Enables Stabilized Zinc Metal Anode.* Advanced Materials Interfaces, 2018. 5(16): p. 1-7.
18. Weixin He, Shiyong Zuo, Xijun Xu, Liyan Zeng, Li Liu, Weiming Zhao, and Jun Liu, *Challenges and strategies of zinc anode for aqueous zinc-ion batteries.* Materials Chemistry Frontiers, 2021. 5(5): p. 2201-2217.
19. Yu Wang, Yani Liu, Haoqiang Wang, Shuming Dou, Wei Gan, Lijie Ci, Yan Huang, and Qunhui Yuan, *MOF-based ionic sieve interphase for regulated Zn2+ flux toward dendrite-free aqueous zinc-ion batteries.* Journal of Materials Chemistry A, 2022. 10(8): p. 4366-4375.
20. C. Yin, C. Pan, X. Liao, Y. Pan, and L. Yuan, *Coordinately Unsaturated Manganese-Based Metal-Organic Frameworks as a High-Performance Cathode for Aqueous Zinc-Ion Batteries.* ACS Appl Mater Interfaces, 2021. 13(30): p. 35837-35847.
21. Neha Sharma, Sabine Szunerits, Rabah Boukherroub, Ran Ye, Sorin Melinte,

Musthafa Ottakam Thotiyl, and Satishchandra Ogale, *Dual-Ligand Fe-Metal Organic Framework Based Robust High Capacity Li Ion Battery Anode and Its Use in a Flexible Battery Format for Electro-Thermal Heating.* ACS Applied Energy Materials, 2019. 2(6): p. 4450-4457.

22. Febri Baskoro, Chin-May Ngue, Kristin B. Labasan, Hui Qi Wong, Man-Kit Leung, and Hung-Ju Yen, *Dual‐Ligand Zn‐Based Metal–Organic Framework as Reversible and Stable Anode Material for Next Generation Lithium‐Ion Batteries.* Energy Technology, 2021. 9(11): p. 1-10.
23. Priscilla Rocío-Bautista, Iván Taima-Mancera, Jorge Pasán, and Verónica Pino, *Metal-Organic Frameworks in Green Analytical Chemistry.* Separations, 2019. 6(3): p. 1-21.
24. Zhongcheng Guo, Yimeng Zhang, Jinggang Liu, Bingxue Han, and Gang Li, *Two imidazole multicarboxylate-based MOFs: syntheses, structures and proton conductive properties.* New Journal of Chemistry, 2021. 45(36): p. 16971-16977.
25. R. Liu, T. Yu, Z. Shi, and Z. Wang, *The preparation of metal-organic frameworks and their biomedical application.* International Journal of Nanomedicine, 2016. 11(1): p. 1187-200.
26. Yuanfeng Wu, Xianghai Song, Jiahui Zhang, Siquan Xu, Ningning Xu, Hongmei Yang, Yanan Miao, Lijing Gao, Jin Zhang, and Guomin Xiao, *$Zn_2(C_9H_3O_6)(C_4H_5N_2)(C_4H_6N_2)_3$ MOF as a highly efficient catalyst for chemical fixation of CO_2 into cyclic carbonates and kinetic studies.* Chemical Engineering Research and Design, 2018. 140: p. 273-282.
27. Witri Wahyu Lestari, Wulan Cahya Inayah, Fitria Rahmawati, Larasati Larasati, and Agus Purwanto, *Metal-Organic Frameworks Based on Zinc(II) and Benzene-1,3,5-Tricarboxylate Modified Graphite: Fabrication and Application as an Anode Material in Lithium-Ion Batteries.* Journal of Mathematical and Fundamental Sciences, 2020. 52(1): p. 81-97.
28. D. Huang, Q. Xin, Y. Ni, Y. Shuai, S. Wang, Y. Li, H. Ye, L. Lin, X. Ding, and Y. Zhang, *Synergistic effects of zeolite imidazole framework@graphene oxide composites in humidified mixed matrix membranes on CO(2) separation.* Royal

Society of Chemistry 2018. 8(11): p. 6099-6109.

29. P. Kalyania and A. Anitha, *Refuse Derived Energy - Tea Derived Boric Acid Activated Carbon as an Electrode Material for Electrochemical Capacitors.* Portugaliae Electrochimica Acta, 2013. 31(3): p. 165-174.

30. X. Zhang, Q. Zhang, J. Reng, Y. Lin, Y. Tang, G. Liu, P. Wang, and G. P. Lu, *N, S Co-Coordinated Zinc Single-Atom Catalysts for N-Alkylation of Aromatic Amines with Alcohols: The Role of S-Doping in the Reaction.* Nanomaterials (Basel), 2023. 13(3): p. 1-11.

31. Yiyang Liu, Liqun Kang, Xu Lu, Paul R. Shearing, Waqar Ahmed, Guanjie He, and Dan J. L. Brett, *MOF-based nanomaterials for zinc-based battery cathodes*, in *Metal-Organic Framework-Based Nanomaterials for Energy Conversion and Storage*. 2022. p. 315-340.

32. M. F. Lagadec, R. Zahn, S. Müller, and V. Wood, *Topological and network analysis of lithium ion battery components: the importance of pore space connectivity for cell operation.* Energy & Environmental Science, 2018. 11(11): p. 3194-3200.

33. Anna A. Kotova, Didier Thiebaut, Jérôme Vial, Antoine Tissot, and Christian Serre, *Metal-organic frameworks as stationary phases for chromatography and solid phase extraction: A review.* Coordination Chemistry Reviews, 2022. 455.

34. Aruuhan Bayaguud, Yanpeng Fu, and Changbao Zhu, *Interfacial parasitic reactions of zinc anodes in zinc ion batteries: underestimated corrosion and hydrogen evolution reactions and their suppression strategies.* Journal of Energy Chemistry, 2022. 64: p. 246-262.

35. Aftab Ahmad, Sadeeq Ullah, Abrar Khan, Waqas Ahmad, Arif Ullah Khan, Usman Ali Khan, Aziz Ur Rahman, and Qipeng Yuan, *Graphene oxide selenium nanorod composite as a stable electrode material for energy storage devices.* Applied Nanoscience, 2019. 10(4): p. 1243-1255.

36. Fangxi Xie, Huan Li, Xuesi Wang, Xing Zhi, Dongliang Chao, Kenneth Davey, and Shi‐Zhang Qiao, *Mechanism for Zincophilic Sites on Zinc‐Metal Anode Hosts in Aqueous Batteries.* Advanced Energy Materials, 2021. 11(9): p. 1-8.

37. Yongling An, Yuan Tian, Yuan Li, Chuanliang Wei, Yuan Tao, Yongpeng Liu,

Baojuan Xi, Shenglin Xiong, Jinkui Feng, and Yitai Qian, *Heteroatom-doped 3D porous carbon architectures for highly stable aqueous zinc metal batteries and non-aqueous lithium metal batteries.* Chemical Engineering Journal, 2020. 400(1): p. 1-12.

VITA

NAME	Penwuanna Arin
DATE OF BIRTH	29 July 1999
PLACE OF BIRTH	Chiang Mai, Thailand
INSTITUTIONS ATTENDED	B.Eng Chemical Engineering, Faculty of Engineering, Srinakharinwirot University
HOME ADDRESS	102/185, Ban Sang Subdistrict, Bang Pa-in District, Phra Nakhon Si Ayutthaya 13170